J Physiol 586.20 (2008) pp 4793–4813

The Journal of Physiology

Internalized Kv1.5 traffics via Rab-dependent pathways

Alireza Dehghani Zadeh, Hongjian Xu, Matthew E. Loewen, Geoffrey P. Noble, David F. Steele and David Fedida

Department of Anaesthesiology, Pharmacology and Therapeutics, University of British Columbia, 2350 Health Sciences Mall, Vancouver, British Columbia, Canada V6T 1Z3

Little is known about the postinternalization trafficking of surface-expressed voltage-gated potassium channels. Here, for the first time, we investigate into which of four major trafficking pathways a voltage-gated potassium channel is targeted after internalization. In both a cardiac myoblast cell line and in HEK293 cells, channels were found to internalize and to recycle quickly. Upon internalization, Kv1.5 rapidly associated with Rab5-and Rab4-positive endosomes, suggesting that the channel is internalized via a Rab5-dependent pathway and rapidly targeted for recycling to the plasma membrane. Nevertheless, as indicated by colocalization with Rab7, a fraction of the channels are targeted for degradation. Recycling through perinuclear endosomes is limited; colocalization with Rab11 was evident only after 24 h post-surface labelling. Expression of dominant negative (DN) Rab constructs significantly increased Kv1.5 functional expression. In the myoblast line, Rab5DN increased Kv1.5 current densities to 1305 ± 213 pA pF^{-1} from control 675 ± 81.6 pA pF^{-1}. Rab4DN similarly increased Kv1.5 currents to 1382 ± 155 pA pF^{-1} from the control 522 ± 82.7 pA pF^{-1} at +80 mV. Expression of the Rab7DN increased Kv1.5 currents 2.5-fold in HEK293 cells but had no significant effect in H9c2 myoblasts, and, unlike the other Rab GTPases tested, over-expression of wild-type Rab7 decreased Kv1.5 currents in the myoblast line. Densities fell to 573 ± 96.3 pA pF^{-1} from the control 869 ± 135.5 pA pF^{-1}. The Rab11DN was slow to affect Kv1.5 currents but had comparable effects to other dominant negative constructs after 48 h. With the exception of Rab11DN and nocodazole, the effects of interference with microtubule-dependent trafficking by nocodazole or p50 overexpression were not additive with the Rab dominant negatives. The Rab GTPases thus constitute dynamic targets by which cells may modulate Kv1.5 functional expression.

(Resubmitted 16 August 2008; accepted 26 August 2008; first published online 28 August 2008)
Corresponding author D. Fedida: Department of Anaesthesiology, Pharmacology and Therapeutics, University of British Columbia, 2350 Health Sciences Mall, Vancouver, British Columbia, Canada V6T 1Z3.
Email: fedida@interchange.ubc.ca

A great deal is known of the biophysical properties of voltage-gated potassium channels and their pharmacological manipulation. However, little is known about the mechanisms that regulate the expression of these channels at the cell surface and the intracellular pathways through which these channels are trafficked. Changes in gene expression have been demonstrated to influence surface expression of the channels, as have associations with accessory subunits, some of which act as chaperones, shepherding newly synthesized channels to the cell surface (reviewed in Steele *et al.* 2007). Once inserted into the plasma membrane, the channels must sooner or later be internalized and targeted either for degradation or for recycling to the cell surface. Internalization of at least some channels is regulated by tyrosine phosphorylation (Holmes *et al.* 1996; Fadool *et al.* 1997; Nesti *et al.* 2004), and is dynamin dependent (Nesti *et al.* 2004; Choi *et al.* 2005). The process is known also to be influenced by dynein motor function (Choi *et al.* 2005), but beyond this limited understanding, the fates of the internalized channels have remained, to date, largely unknown.

Among the prime candidates for the proximal regulators of Kv1.5 internalization and trafficking are the Rab GTPases. These proteins are intimately involved in the regulation of vesicle trafficking in all eukaryotic cells (Zerial & McBride, 2001), including budding, delivery, tethering and fusion (reviewed in Grosshans *et al.* 2006). Rab5, for example, is required for clathrin-mediated endocytosis and is essential to early endosome formation and maturation. Rab4 associates with at least a subset of early endosomes and is involved mainly in fast recycling

DOI: 10.1113/jphysiol.2008.161570

to the plasma membrane. Rab11 is essential to another recycling pathway and is also involved in the trafficking of many membrane proteins from the Golgi to the cell surface. Rab7, on the other hand, is associated with the late endosome and trafficking of cargo to the lysosome for degradation. All of these Rab GTPases are expressed in cardiomyocytes (Kessler *et al.* 2000; Odley *et al.* 2004; Filipeanu *et al.* 2006; Liu & Askari, 2006).

Rab5 and Rab11 have been implicated in the trafficking of KCNQ1/KCNE1 (Seebohm *et al.* 2007), and dominant negative Rab4 and Rab11 mutants have been reported to reduce the apparent surface fluorescence of tagged Kv1.5 (McEwen *et al.* 2007). Here, we describe the association of Kv1.5 with all of Rab5, Rab4, Rab11 and Rab7 following internalization in a rat cardiac myoblast cell line and in HEK293 cells. In addition to live- and fixed-cell imaging experiments, the effects of dominant negative Rab mutants on the functional expression of the channel were investigated. We demonstrate that a substantial portion of the internalized Kv1.5 recycles rapidly to the plasma membrane, very probably via a Rab4-dependent pathway, and that another portion is shuttled to the late endosome for degradation. We further demonstrate that all of this trafficking is dependent upon a functional dynein motor. These findings establish a framework for examining the regulation of Kv1.5 surface expression in health and disease.

Methods

Materials

The wild-type and dominant negative Rab clones were a kind gift of Dr T. Hebert and Dr Denis Dupre, McGill University, Montréal, Canada. pcDNA3-EGFP(N) (Enhanced Green Fluorescent Protein) was made by performing PCR on pEGFP-N1 (Invitrogen) using primers 5′-GTAAGCTTATGGTGAGCAAGGGCGAGGAGC-3′ and 5′-CAGAATTCCTTGTACAGCTCGTCCATGCCG-3′, and the product was inserted between the *Hin*dIII and *Eco*RI sites of pcDNA3 (Invitrogen). pcDNA3-mCherry(N) was made by performing PCR on mCherry template using primers 5′-GTAAGCTTATGGTGAGCAAGGGCGAGGAGG-3′ and 5′-CAGAATTCCTTGTACAGCTCGTCCATGCG-3′ and inserted between the *Hin*dIII and *Eco*RI sites of pcDNA3 (Invitrogen). Rab7A WT and Rab7A N125I (Rab7DN) were cloned as *Hin*dIII–*Xho*I fragments into pBluescript SK(+). The Rab7 clones were then transferred as *Apa*I–*Xba*I fragments into pcDNA3-EGFP(N). In constructing the Rab4, Rab5 and Rab11 fusion proteins, Rab constructs were cloned into pcDNA3-EGFP(N) as *Eco*RI–*Xho*I fragments. Rab5WT and Rab5S34N (Rab5DN) with appropriate restriction sites for the purpose were generated by PCR amplification using primers 5′-CACTCGAGTTAGATGTTCTGACAGCA-3′. p50/dynamitin was PCR amplified using primers 5′-GTGAATTCATGGCGGACCCTAAATACG-3′ and 5′-CACTCGAGTCACTTTCCCAGCTTCTTC-3′ and subcloned into both pcDNA3EGFP(N) and pcDNA3-mCherry(N). pcDNA3-EGFP(C) was created by subcloning EGFP, including its stop codon, between the *Eco*RI and *Xho*I sites of pcDNA3 and was used for control experiments. pcDNA3-Kv1.5-HA (Hemagglutinin) was generated by inserting the coding sequence for the nine-amino-acid residue HA tag flanked by single glycine codons into the coding sequence of Kv1.5 between residues 307 and 308. pcDNA3-Kv1.5-mCherry(N) was created by subcloning Kv1.5 into *Eco*RI–*Xho*I site of pcDNA3-mCherry(N).

Nocodazole was purchased from Sigma, reconstituted in DMSO and applied to cell media to a final concentration of 35 μM. Cycloheximide and botulinum toxin C were purchased from Sigma. Mouse anti-HA clone (12CA5) was from Roche. Rabbit anti-HA was from Zymed Laboratories Inc. (South San Francisco, CA, USA). Alexa Fluor-conjugated secondary antibodies were purchased from Molecular Probes. Goat anti-mouse Fab fragments conjugated to Rhodamine Red-X was from Jackson ImmunoResearch Laboratories Inc. (West Grove, PA, USA). The mouse mAb to canine LAMP-2 (*AC17*) (Nabi *et al.* 1991) was a gift from Dr R. Nabi (University of British Columbia).

Cell preparation and transfection

All cell culture supplies were obtained from Invitrogen (Mississauga, ON, Canada). H9c2 rat cardiac myoblasts transiently transfected with Kv1.5-HA and a stable line of HEK293 cells expressing Kv1.5 were used in electrophysiology experiments. Transient transfections were performed with cells that had been plated at 20–30% confluency on sterile coverslips in 25 mm Petri dishes one day prior to transfection. Two micrograms of EGFP DNA was transfected as control, whereas 2–3 μg wild-type or dominant negative mutant EGFP-tagged Rab-encoding DNA was transfected as the experimental group, respectively. In experiments using H9c2 cells, mCherry-tagged Kv1.5 DNA was cotransfected with the respective dominant negative Rab DNA. Transfections were carried out using 1 μl of lipofectamine 2000 (Invitrogen) in 400 μl of Opti-MEM mixed with the transfection DNA sample and added to the cells after replacing the media with 1 ml of minimal essential medium (MEM). After 5–6 h, the medium was replaced with MEM supplemented with 10% fetal bovine serum (FBS) and the cells were grown at 37°C in an air–5% CO_2 incubator. Recordings were conducted 24 or 48 h after transient transfection.

Live cell imaging

For live imaging assays, HEK cells stably expressing Kv1.5-HA were seeded on plain coverslips placed in Sykes–Moore chambers, transfected and labelled with mouse-anti-HA (Roche) on ice for 1 h. They were then washed and labelled with goat antimouse Fab fragments conjugated to Rhodamine Red-X (Jackson Immuno Research Laboratories Inc.) for 1 h on ice. Cells were then washed 3 times with cold medium and live-imaged using a 63× Apochromat water immersion objective with an Olympus Fluoview 1000 confocal microscope equipped with a heated box at 37°C. Conjugated Fab fragments of secondary antibodies were used because bivalent secondary antibodies appeared to be inducing crosslinking of Kv1.5 proteins, causing the formation of large fluorescent patches on the cell membrane. These patches were not seen when the conjugated Fab fragments were employed. Image analysis was performed using ImageJ software (NIH).

Recycling assay

HEK293 cells stably expressing Kv1.5-HA were cultured as described above. After 24 h, the cells were labelled with Mouse-α-HA (Roche) for 30 min on ice, washed with cold culture medium, and incubated at 37°C for 30 min to allow internalization of labelled Kv1.5-HA. For control cells, in which recycling was blocked by botulinum toxin, cells were treated in exactly the same way except that 10 nM botulinum toxin C was added to the medium for 1 h prior to labelling. The cells were then incubated for a further 30 min on ice with saturating amounts of goat anti-mouse Fab fragments conjugated to Rhodamine Red-X, washed and placed at 37°C for various times to allow recycling of internalized labelled Kv1.5-HA to the plasma membrane. The cells were then placed back on ice and stained with goat anti-mouse Alexa488 conjugated antibody for 30 min in order to label only the subpopulation consisting of the recycled Kv1.5 molecules. Cells were then fixed and mounted in DABCO/glycerol and imaged using an Olympus FV1000 confocal microscope equipped with a 60× (NA, 1.4) oil-immersion objective. The sample at $t = 120$ s was used to adjust the acquisition settings of the microscope and the same settings were applied for acquiring images at all time points. Sectioning with a z distance of 1 μm was performed for each cell. Images were processed using ImageJ. Background signal was subtracted for each fluorescence signal.

For Rab4DN coexpression experiments, the procedure was as above with the following modifications: HEK293 cells stably expressing Kv1.5-HA were transfected with pcDNA3-Rab4DN-EGFP, and the recycling assay was performed 24 h later. In the staining procedure, Alexa647 conjugated goat anti-mouse was used instead of Alexa488 to detect the recycled Kv1.5. Three consecutive slices that were representative of each cell were chosen and Alexa647 fluorescence intensity per unit of length (micrometer) along the membrane was measured using ImageJ.

Kv1.5 internalization and colocalization assay

For surface labelling of Kv1.5, HEK cells stably expressing Kv1.5-HA and transfected with one of Rab4WT, Rab5WT, Rab7WT, or Rab11WT were labelled with mouse-anti-HA antibody (Roche) for 1 h on ice, washed 3 times with cold culture medium, then incubated at 37°C for various times to allow internalization of labelled Kv1.5-HA. The cells were then fixed with 4% paraformaldhyde (final concentration) and permeabilized in phosphate buffered saline (PBS) containing 0.1% Triton X-100, and non-specific binding was blocked by incubation in 2% BSA in PBS for 30 min at room temperature. Following this, the cells were labelled with Alexa594 conjugated goat anti-mouse antibody (Molecular Probes) for 1 h, washed and mounted using DABCO/glycerol. Preliminary experiments showed that the EGFP fluorescence survives the fixation and staining procedure and colocalized quantitatively with anti-GFP antibody fluorescence (Chemikon) (data not shown). EGFP signal was therefore routinely used in imaging EGFP-tagged proteins in fixed cells. Samples were imaged and analysed as described above. In colocalization assays, the number of Kv1.5-positive vesicles and the number positive for both Kv1.5 and Rab-EGFP were counted.

In lysosomal colocalization assays, HEK293 cells stably expressing Kv1.5-HA were seeded on coverslips overnight. The cells were then transfected with pcDNA3Rab7WT-EGFP and incubated at 37°C for 24 h. Surface Kv1.5 was labelled with rabbit α-HA on ice for 1 h, then washed and moved to 37°C for 30 min to allow internalization of labelled Kv1.5 channels. The cells were then fixed, permeabilized and stained with mouse anti-LAMP2 (AC17) for 1 h at room temperature. The cells were stained with anti-rabbit-Alexa594 and anti-mouse-Alexa647 to detect Kv1.5-HA and lysosomes, respectively.

Transferrin internalization assay

HEK293 cells were seeded on coverslips and incubated at 37°C overnight. The cells were then transfected with pcDNA3-Rab4DN-EGFP. After 24 h, the cells were washed with culture medium, and stained with transferrin conjugated with Alexa Fluor 594 for 5 min at 37°C. The cells were then washed and stained on ice with wheat germ agglutinin conjugated to Alexa Fluor 350 for 10 min to label the cell membrane before fixation. Stacks of images were made using the confocal microscope. Three

representative slices from each cell were chosen and the amount of surface and internalized transferrin in presence or absence of Rab4DN-EGFP was measured using ImageJ software.

Electrophysiological experiments and solutions

Whole-cell current recordings and analyses were carried out using an Axopatch 200B amplifier and pCLAMP10 software (Axon Instruments, Union City, CA, USA). Patch electrodes were pulled from thin-walled borosilicate glass (World Precision Instruments, Sarasota, FL, USA) on a horizontal micropipette puller (Sutter Instruments, CA, USA). Electrodes had resistances of 1–4 MΩ when filled with intracellular solution. Analogue capacity compensation and 80% series resistance compensation were used during whole cell measurements. For current recordings, cells were depolarized between −80 and +80 mV in 10 mV steps from a holding potential of −80 mV. Data were sampled at 10 kHz and filtered at 2 kHz. All whole-cell recordings were performed at room temperature (20–22°C), and control and experimental groups were studied in a blinded manner on the same days. Data are presented as current density by normalizing peak current amplitude to the corresponding cell capacitance value, and represented as means ± S.E.M.

The extracellular solution contained (in mM): 5 KCl, 135 NaCl, 2.8 sodium acetate, 1 $MgCl_2$, 10 Hepes and 1 $CaCl_2$, adjusted to pH 7.4 with NaOH. The intracellular solution used in the pipettes contained (in mM): 130 KCl, 5 EGTA, 1 $MgCl_2$, 10 Hepes, 4 Na_2ATP, and 0.1 GTP, adjusted to pH 7.2 with KOH. For nocodazole experiments, 25 mM nocodazole stock solution was prepared in 100% DMSO and stored at −20°C. Cells were incubated with 35 μM nocodazole for 6 h prior to electrophysiological recordings. DMSO concentrations never exceeded 0.2% v/v in the final experimental solutions.

Data statistics

Results are expressed as means ± S.E.M. Statistical analyses were conducted using Student's *t* test (paired and unpaired) or by one-way ANOVA, as appropriate.

Results

HA-tagged Kv1.5 is expressed normally

The study of Kv1.5 postinternalization trafficking requires the ability to distinguish surface and internalized Kv1.5 from other internal pools of the channel. Therefore, to facilitate our studies, an externally HA-tagged Kv1.5 construct was generated in pcDNA3. In this construct, a nine-amino-acid residue HA tag flanked on each side by a glycine residue was inserted between residues 307 and 308 in the Kv1.5 S1–S2 linker. When expressed in HEK293 cells, the insert had no detectable effect on the magnitude or kinetics of Kv1.5 currents (data not shown). The utility of the clone was confirmed by transfection of HEK293 cells with the construct and thereafter following the fates of the channels expressed on the cell surface, as assayed by live-cell imaging and immunohistochemistry. Surface expression was robust and internalized vesicles were evident within 5 min incubation at 37°C after labelling, which became more prominent by 11 min (Fig. 1*A*). In terms of mobility, these internalized vesicles fell into two general groups. Most vesicles showed little movement over periods of several minutes whereas others were quite mobile. The arrows in Fig. 1*B* highlight the movement of one such vesicle as it moves away from the plasma membrane.

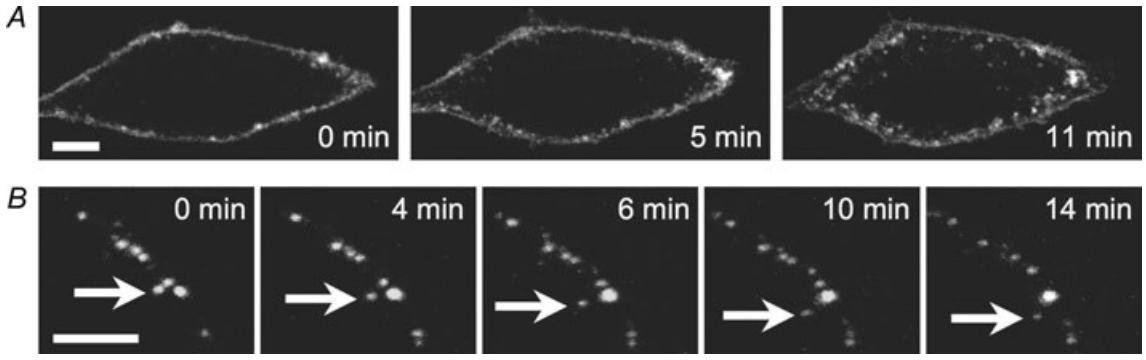

Figure 1. Dynamics of Kv1.5-HA mobility in HEK293 cells
A, Kv1.5-HA labelled by indirect fluorescence staining of live cells is restricted initially to the cell surface (time 0, left) and internalizes rapidly in vesicle-like structures (time 5 and 11 min, middle and right). *B*, variable mobility of internalized Kv1.5-containing vesicles. The highlighted vesicle exhibits retrograde (time 0–6 min) then anterograde movement (time 10–14 min). Scale bar = 5 μm.

Kv1.5 recycles rapidly to the plasma membrane following internalization

Lakadamyali *et al.* (2006) have reported that highly mobile early endosomes are preferentially targeted to the degradation pathway and that the relatively immobile population is generally targeted for recycling to the plasma membrane. It seemed likely therefore that a large portion of internalized Kv1.5 would be returned to the plasma membrane. To investigate whether this was indeed true, a recycling assay was devised. This assay is outlined in Fig. 2*A*. In essence, surface-expressed Kv1.5-HA in HEK cells was bound to anti-HA antibody and then the cells were incubated at 37°C for 30 min to allow some of that labelled Kv1.5 to be internalized. The remaining surface Kv1.5-HA was then labelled on ice with saturating amounts of Rhodamine Red-X conjugated anti-mouse Fab

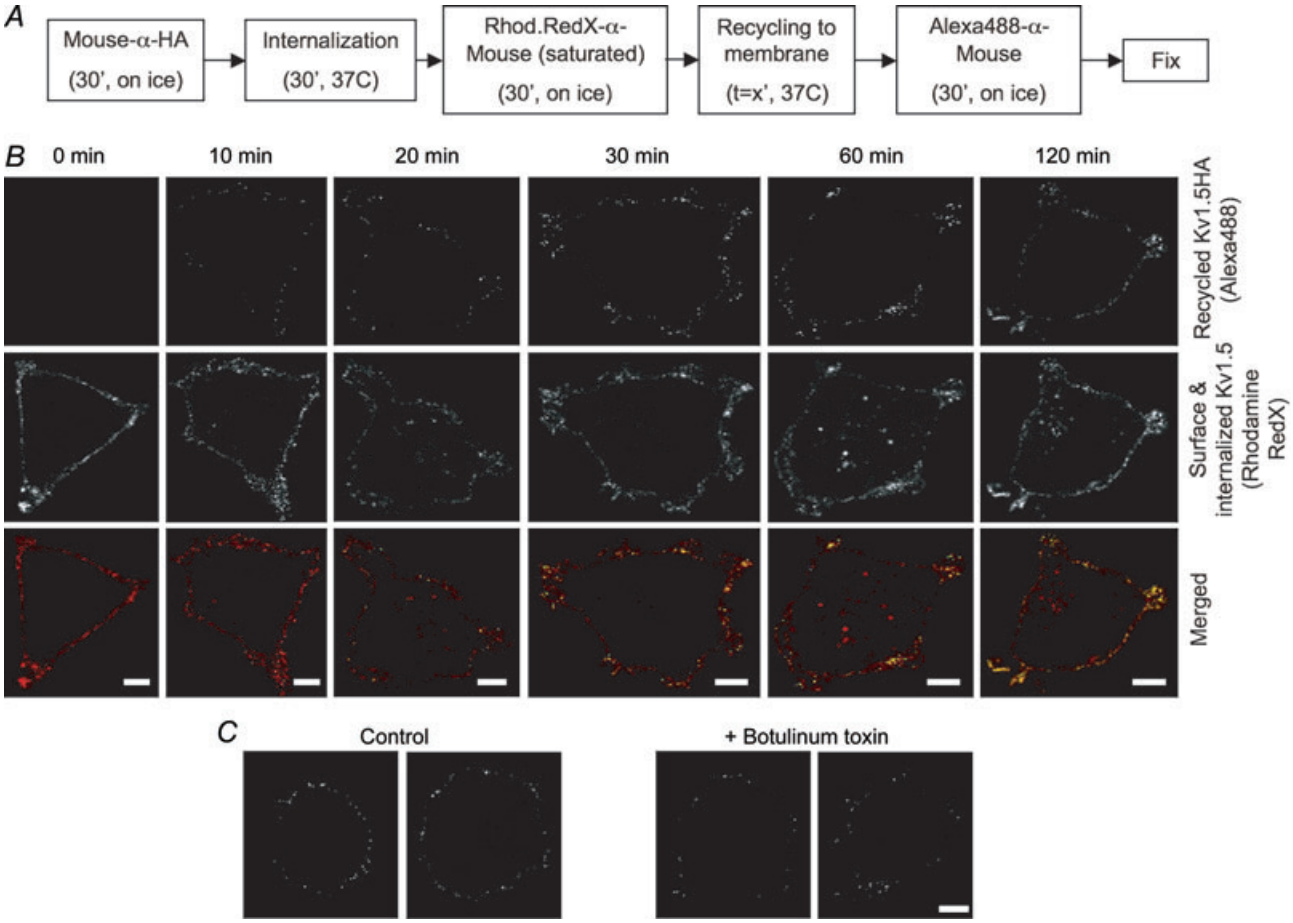

Figure 2. Internalized Kv1.5 rapidly recycles to the plasma membrane
A, schematic representation of the recycling assay protocol. HEK293 cells stably expressing Kv1.5-HA were incubated with mouse anti-HA to tag the surface-expressed channels. Cells were then given 30 min to internalize surface channel thereafter labelled on ice to saturation with Rhodamine Red-X-conjgated anti-mouse to label all remaining anti-HA tagged surface Kv1.5-HA and to block binding of the Alexa Fluor 488-conjugated anti-HA antibody used in the following step. Cells were then incubated for the indicated times to allow recycling, labelled with Alexa Fluor 488-conjugated anti-mouse on ice to detect channels that had recycled to the plasma membrane, then fixed and mounted. *B*, upper panels, Alexa Fluor 488 fluorescence after various recycling times. Recycled Kv1.5-HA is absent on the membrane at 0 min. Binding of Alexa Fluor 488-conjugated antibody, indicative of recycled channels, is evident beginning at 10 min and, in increasing amounts, at all subsequent time points. Middle panels, Rhodamine Red-X fluorescence at the same time points. Surface staining is robust at all times. Fluorescence is apparent also in vesicular compartments at later time points, indicative of continued internalization of the channel. Lower panels, merged images showing combined Rhodamine Red-X and Alexa488 fluorescence (recycled Kv1.5-HA) at the indicated time points. Recycled channel colocalizes with Rhodamine Red-X-labelled channels and therefore appears yellow in these images. *C*, botulinum toxin reduces recycling of Kv1.5. Recycling is assayed as Alexa Fluor 488 fluorescence as in *B* above. The recycling assay was performed as described in Methods in the presence (right panels) or absence (left panels) of 10 nM botulinum toxin C after 30 min recycling time. Scale bar = 5 μm.

fragment. This labels all of the anti-HA bound channels at the surface but internalized anti-HA bound Kv1.5 is left unlabelled. To assay the return of that internalized fraction to the plasma membrane, the cells were then incubated for various times at 37°C and thereafter stained with Alexa Fluor 488-conjugated anti-mouse on ice. Thus, the channels that remained at the surface during the internalization period are labelled by Rhodamine Red-X. Only channels that were internalized, and thus protected from the Rhodamine labelling, and that then recycled to the cell surface are labelled by the Alexa Fluor 488. As illustrated in Fig. 2*B*, this assay detected rapid and robust recycling of the channel. No Alexa Fluor 488 fluorescence, indicative of recycled channels, was evident at time 0, but by 10 min, punctate foci appeared on the cell surface, indicating that previously internalized anti-HA tagged Kv1.5 was reappearing at the cell surface (Fig. 2*B*, upper panels). The numbers of these foci increased over time such that, by 2 h, Alexa Fluor 488 fluorescence was extensive. Rhodamine Red-X staining at the membrane was extensive at all times (middle panels), indicating that Kv1.5 has a net surface residency time of greater than 120 min. At longer incubation times, Rhodamine Red-X staining appeared also in internal vesicles, indicating that Kv1.5 internalization continued throughout the recycling incubation.

Block of recycling by treatment of cells with botulinum toxin C for 1 h prior to conducting the recycling assay reduced Alexa 488 staining by over 50% (Fig. 2*C*). After 30 min recycling time, Alexa Fluor 488 fluorescence intensity was 4415 ± 869 fluorescence intensity units per micrometre of plasma membrane length ($n = 15$ cells) in botulinum toxin-treated cells, whereas the signal was 9232 ± 510 per micrometre in the untreated cells ($n = 15$ cells; $P < 0.001$). Antibody exchange, thus, cannot explain the majority of the recycled channel signal; the recycling assay provides a reliable measure of channel internalization and recycling. Internalized Kv1.5 clearly recycles efficiently to the plasma membrane.

Internalized Kv1.5 associates with Rab5

There are multiple routes via which internalized channels may traffic and recycle. To define the transport pathways for internalized Kv1.5, we investigated the involvement of specific Rab GTPases in the trafficking of the channel. Rab GTPases define the various intracellular trafficking vesicles, regulating the formation of these compartments and recruiting the various effectors required for their function (Pfeffer, 2001). We began these studies by examining the role of Rab5 in Kv1.5 internalization. Rab5 is required for clathrin-mediated endocytosis and early endosome formation (Bucci *et al.* 1992) and recruits EEA1 to these vesicles (Simonsen *et al.* 1998; Christoforidis *et al.* 1999). A schematic diagram highlighting the role of Rab5 in the internalization/recycling pathways is presented in Fig. 3*C*.

The role of Rab5 in Kv1.5 trafficking was tested in HEK293 cells and in a rat cardiac myoblast cell line, H9c2. Surface Kv1.5-HA was labelled with anti-HA and, after incubation for 0–60 min at 37°C, cells were fixed, permeabilized, and stained with Alexa Fluor 594-conjugated secondary antibody. The cells were then imaged under a confocal microscope. Within 5 min of labelling, a substantial fraction of internalized Kv1.5 was found to colocalize in vesicles with Rab5 (Fig. 3*A*). 38.1% (72 of 214) of Kv1.5 positive vesicles in 8 cells unequivocally harboured Rab5 (Fig. 3*B*). Colocalization declined to about 11% of Kv1.5-HA positive vesicles after 1 h of postlabelling incubation. Similar colocalization was detected in H9c2 myoblast cells cotransfected with Kv1.5-HA and Rab5-EGFP (Fig. 3*D*).

To test whether Rab5 influences Kv1.5 functional expression, electrophysiological experiments were performed. A Rab5 dominant negative (Rab5 S34N; Rab5DN) mutant was also employed. EGFP-tagged wild-type and dominant negative Rab5 constructs were overexpressed individually in H9c2 myoblasts cotransfected with mCherry-tagged Kv1.5 and in HEK293 cells stably expressing Kv1.5. mCherry-Kv1.5 channel is fully functional; its kinetics are like wild-type (data not shown). Transfection with the wild-type Rab protein had no effect on Kv1.5 currents in either cell type but coexpression of the Rab5 dominant negative substantially increased current densities. In the myoblasts (Fig. 4*A* and *B*), current densities at +80 mV were 675 ± 81.6 pA pF^{-1} ($n = 8$) in the EGFP-transfected controls and 1305 ± 213 pA pF^{-1} ($n = 9$) in the Rab5DN-expressing cells. Similarly in the HEK293 cells, Kv1.5 currents were tripled from the EGFP-transfected control densities of 561 ± 97.2 pA pF^{-1} ($n = 17$) to 1693 ± 306 pA pF^{-1} in the Rab5DN-expressing cells (Fig. 4*C* and *D*).

To test whether the Rab5DN-induced increase in currents was related to the same Kv1.5-trafficking pathway in which dynein functions, we determined whether the effects of the dominant negative were additive with those of p50 over-expression. Over-expression of p50/dynamitin, a component of the dynein/dynactin complex, also increases Kv1.5 surface expression, very probably by interfering with early endosome trafficking (Choi *et al.* 2005). p50 over-expression blocks the binding of dynein to its cargoes, thereby blocking retrograde trafficking (Echeverri *et al.* 1996; Burkhardt *et al.* 1997). Rab5DN and p50 over-expression each more than doubled Kv1.5 current densities in the Kv1.5-expressing HEK293 cells compared with the EGFP-transfected control (Fig. 4*E*). Kv1.5 current densities in control averaged 661 ± 110 pA pF^{-1} ($n = 13$) at +80 mV. Rab5DN increased these densities

to 1429 ± 148 pA pF^{-1} ($n = 10$) and p50 similarly increased Kv1.5 densities to 1178 ± 114 pA pF^{-1}. When p50 and Rab5DN were transfected together into the cells, there was no additivity. Current density at 1142 ± 143 pA pF^{-1} was not significantly different from that in cells expressing p50 or the Rab5-DN alone (Fig. 4*E*). Similar results were obtained when the microtubule-depolymerizing agent nocodazole was used instead to block microtubule-dependent trafficking (Fig. 4*F*).

Finally, we assayed the internalization of Kv1.5 in control cells and in cells transfected with the Rab5DN. HEK293 cells stably expressing Kv1.5-HA were left untransfected or were transfected with Rab5DN-EGFP. Twenty-four hours later, the cells were labelled with mouse anti-HA, then incubated at 37°C for 30 min to allow internalization. Unlike wild-type Rab5, Rab5DN staining did not localize to vesicles; instead, like all the Rab dominant negatives tested (see below), expression was diffuse throughout the cytoplasm. The number of Kv1.5-positive vesicles in the cells coexpressing the Rab5DN was counted and compared to the number in the untransfected cells. In the presence of the Rab5DN, fewer vesicles containing Kv1.5 were evident in the interior of the cells (Fig. 5*A*). As quantified in Fig. 5*B*, the Rab5DN construct reduced the number of Kv1.5-positive vesicles by 50% relative to control ($P < 0.01$). Thus, it is highly likely that the Rab5DN, like p50, increases Kv1.5 surface expression by interfering with endocytosis of the channel.

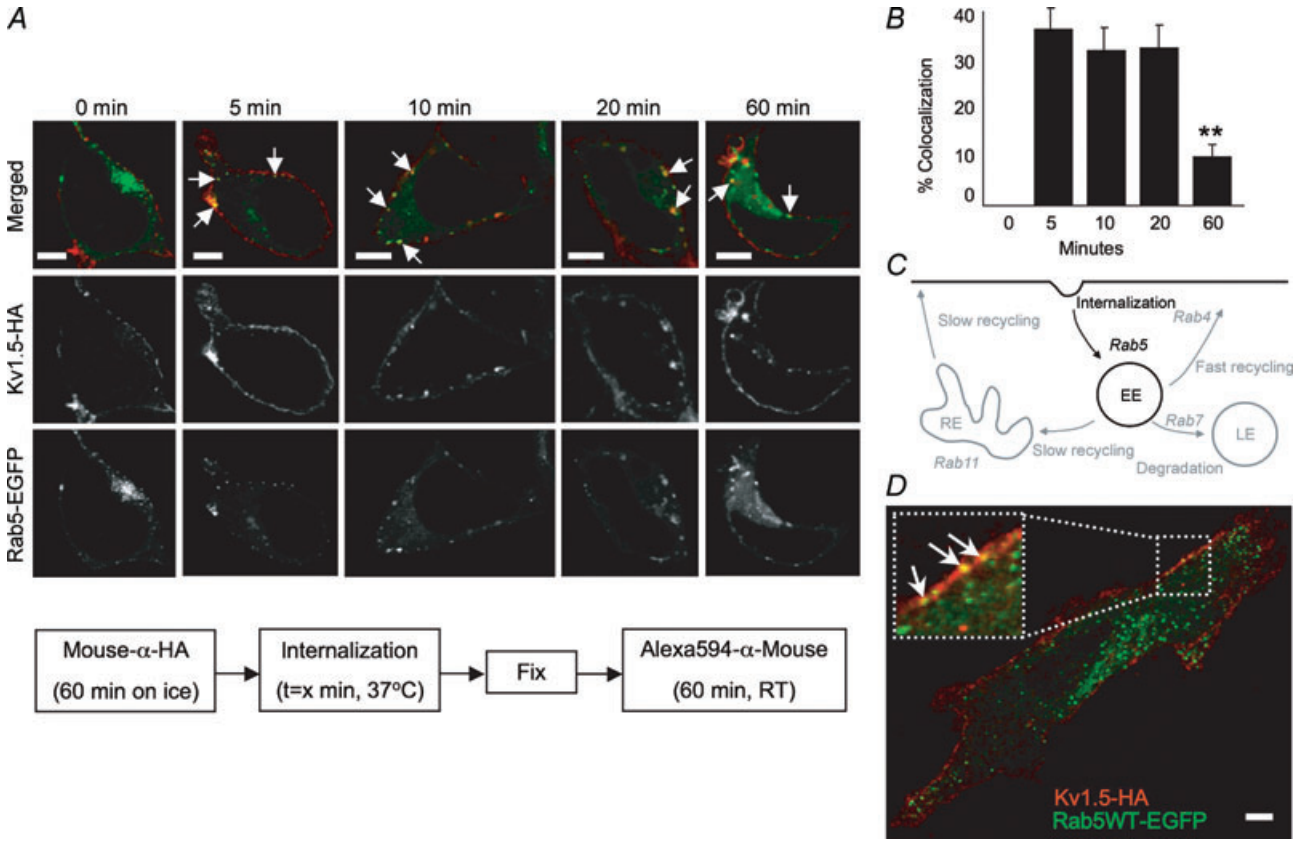

Figure 3. Kv1.5 colocalizes rapidly with the Rab5 GTPase in HEK293 cells and H9c2 myoblasts
A, time series of internalized Kv1.5 colocalization with Rab5. Upper panels, merged Rab5-EGFP and Kv1.5-HA associated fluorescence at the indicated time points. The arrows highlight some of the vesicles in which Kv1.5 and Rab5 are seen to colocalize. Middle panels, Kv1.5-HA associated Alexa Fluor 594 fluorescence alone. Only channels that were present at the cell surface at the beginning of the experiment are labelled. Lower panels, Rab5-EGFP fluorescence alone. The schematic diagram below outlines the protocol employed in these experiments. *B*, quantification of Rab5 colocalization in Kv1.5-positive vesicles. Percentage colocalization was calculated from the fraction of Kv1.5 positive vesicles in the imaged cells that were found to exhibit also tagged-Rab5 EGFP fluorescence. $^{**}P < 0.01$, one-way ANOVA. *C*, schematic representation of the roles of Rab5, Rab4, Rab11 and Rab7 in membrane protein endocytosis and recycling. The Rab5-dependent steps are highlighted in this figure. EE, early endosome; RE, recycling endosome; LE, late endosome. *D*, Kv1.5-HA and Rab5-EGFP colocalize in H9c2 cells after 20 min internalization time. Experimental protocol was as in *A*. Arrows in the magnified inset highlight some of the vesicles in which Kv1.5 and Rab5 are seen to colocalize. Scale bar = 5 μm

Internalized Kv1.5 quickly associates with Rab4, a marker for fast recycling

Once internalized, a membrane protein may be shunted along a number of paths. It may be recycled to the plasma membrane through either a fast or a slow pathway, or it may be sent to the lysosome for degradation (Fig. 6*C*). Many proteins, KCNQ1 for example (Seebohm *et al.* 2007), recycle in a Rab11-dependent manner via the perinuclear recycling endosome. Others, like the transferrin receptor, mainly skip this endosome and return to the plasma membrane directly from the early endosome in a Rab4-dependent process (Sheff *et al.* 2002). To investigate whether internalized Kv1.5 follows either or both of these pathways, we assayed colocalization of internalized channel with the EGFP-tagged Rab4 and Rab11 proteins.

Results from immunocytochemistry/confocal microscopy experiments assaying colocalization of Kv1.5 with Rab4 are shown in Fig. 6. Colocalization of Kv1.5 and Rab4 was evident within 10 min of internalization and remained evident at the 20 and 60 min time points tested (Fig. 6*A*). Quantification of the colocalization showed that 73 of 324 vesicles (22.5%) harbouring Kv1.5 in 20 cells were unequivocally Rab4 positive after 10 min internalization time. Colocalization remained robust through at least 20 min postinternalization before declining (Fig. 6*B*). Colocalization was robust, also, 20 min after internalization, in H9c2 myoblasts cotransfected with Kv1.5-HA and Rab4-EGFP (Fig. 6*D*).

Electrophysiological experiments confirmed Rab4 involvement in modulating Kv1.5 surface expression (Fig. 7). Co-expression of an EGFP-tagged Rab4 dominant

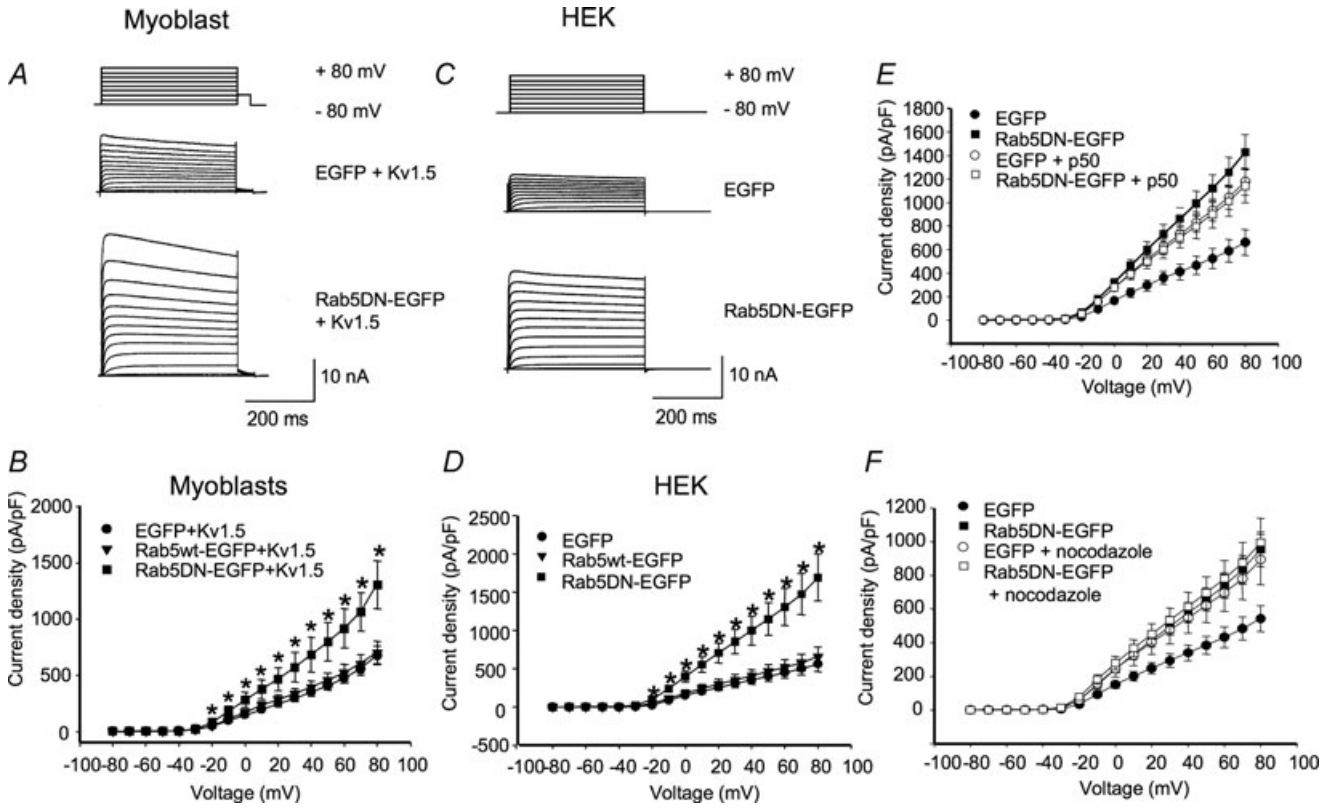

Figure 4. Effect of Rab5 wild-type overexpression and Rab5 dominant negative (Rab5DN) expression on Kv1.5 currents

Cells were depolarized from −80 to +80 mV in 10 mV, 500 ms steps). H9c2 cells were repolarized to −40 mV for 50 ms then to −80 mV and HEK293 cells were repolarized directly to −80 mV between pulses. Data are represented as means ± S.E.M. Current densities from control cells (EGFP), Rab5-EGFP and Rab5DN-EGFP transfected cells are plotted against voltage. *A* and *C*, sample traces of control and Rab5DN-transfected H9c2 and HEK293 cells, respectively. The HEK293 line stably expresses Kv1.5; H9c2 cells were cotransfected with Kv1.5-mCherry. *B* and *D*, current density *versus* voltage plot for data recorded 24 h post-transfection for H9c2 and HEK293 cells, respectively. *E*, effect of p50/dynamitin overexpression on Kv1.5 current density in control and Rab5DN-coexpressing HEK293 cells. Current recordings were performed 36–48 h post-transfection. *F*, current densities of control cells and Rab5DN-EGFP transfected cells with or without nocodazole treatment are plotted against voltage. Nocodazole-treated cells were incubated with 35 μM nocodazole for 6 h prior to electrophysiological recording. $^*P < 0.05$, one-way ANOVA.

negative (Rab4 N121I; Rab4DN) with Kv1.5-mCherry in H9c2 myoblasts and Rab4DNEGFP in HEK293 cells stably expressing Kv1.5 significantly increased Kv1.5 functional expression (Fig. 7*A–D*). Control current densities at +80 mV were 522 ± 82.7 ($n = 7$) and 488 ± 68.0 pA pF^{-1} ($n = 23$) in the myoblasts and HEK293 cells, respectively, rising to 1382 ± 155 ($n = 7$) and 1095 ± 87.4 pA pF^{-1} ($n = 14$), respectively, in the Rab4DN-expressing cells. Similar to Rab5, over-expression of Rab4 wild-type protein itself had no effect on Kv1.5 current levels in the HEK cells (Fig. 7*D*). In the myoblast line, however, the Rab4 wild-type construct increased Kv1.5 current densities to 869 ± 136 ($n = 8$) (Fig. 7*B*). Perhaps Rab4 levels normally limit recycling in these cells, and thus recycling is facilitated by the overexpression of the wild-type construct. Overall, these results strongly support a role for Rab4-dependent Kv1.5 recycling to the plasma membrane after channel internalization.

That Kv1.5 currents were increased by coexpression of the Rab4DN was surprising since Rab4 function is required for rapid recycling to the plasma membrane (Zerial & McBride, 2001). As expected, the Rab4DN did reduce the return of labelled channel to the plasma membrane (Fig. 8). Using a recycling assay similar to that described above, except that Alexa647-conjugated anti-mouse was used to detect the recycled channels, we determined that the dominant negative reduced rapid recycling by about 40%. Lower pixel intensities from Alexa Fluor 647 fluorescence in cells expressing Rab4DN indicated that fewer internalized channels returned to the surface (Fig. 8*A*). Kv1.5 recycling was reduced to 62 ± 16% of control levels after 20 min recycling time (Fig. 8*B*). At 30 min, recycling was similarly reduced to 58 ± 17% of control and, at 60 min, to 61 ± 21% of control levels. This reduction was significant in all cases ($P < 0.05$). Thus, Rab4DN is clearly interfering with the recycling of the channel. Another phenomenon must underlie the paradoxically increased functional expression of the channel seen when this Rab4 mutant is coexpressed with Kv1.5.

One possibility is that the Rab4 dominant negative somehow causes a large increase in the insertion of newly synthesized Kv1.5 into the plasma membrane. Under this scenario, this increase in incorporation of new channel would necessarily more than compensate for the reduction in channel recycling. To test this possibility, we treated Kv1.5-expressing HEK293 cells that had been transfected with the Rab4DN with 100 μg ml^{-1} cycloheximide for 6 h immediately prior to electrophysiological recording. Cycloheximide blocks the synthesis of new protein and, thus, should deprive the cell of new channels that could be inserted into the plasma membrane. As shown in Fig. 9*A* and *B*, this treatment did not interfere with the Rab4DN-associated increase

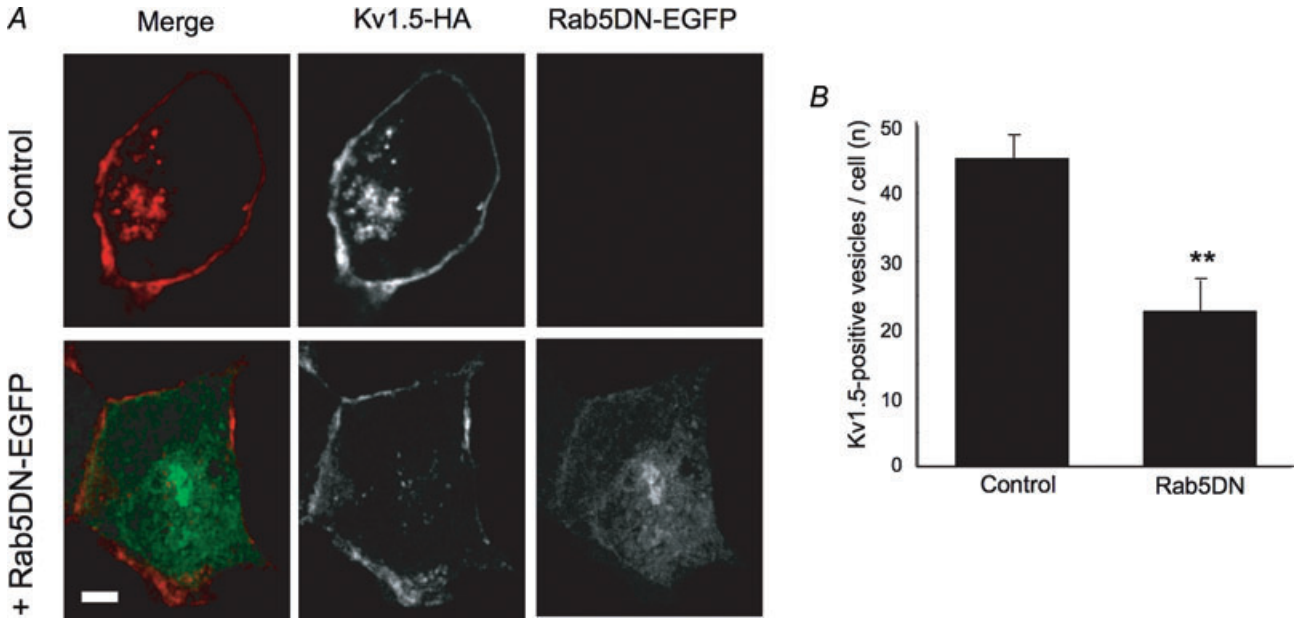

Figure 5. Co-expression of Rab5DN reduces Kv1.5 internalization
A, representative images showing internalized Kv1.5-HA (red; Alexa Fluor 594-conjugated) positive vesicles in control (upper panels) and Rab5DN-EGFP-transfected cells (lower panels). Only channels that were present at the cell surface at the beginning of the experiment are labelled. The number of Kv1.5-positive internalized vesicles is noticeably lower in the Rab5DN-expressing cells (middle panel, lower) than in the control, untransfected cells. Scale bar = 5 μm. *B*, number of Kv1.5-positive vesicles per cell under control conditions and when Rab5DN is coexpressed. $^{**}P < 0.01$, Student's *t* test.

in Kv1.5 functional expression. Rab4DN increased Kv1.5 currents relative to control, untransfected cells irrespective of the presence of cycloheximide in the medium (Fig. 9*B*). Control current densities at +80 mV were 238.1 ± 60.2 pA pF^{-1} and 324.0 ± 58.2 pA pF^{-1} in untreated and cycloheximide-treated cells, respectively. In cells coexpressing Rab4DN, the densities were 859.7 ± 208.8 pA pF^{-1} in the absence of cycloheximide and 746.5 ± 248.8 pA pF^{-1} in the presence of the drug.

Another possibility is that block of the Rab4-dependent recycling pathway may indirectly interfere with endocytosis. Interference with another step downstream of endocytosis, dynein-dependent retrograde trafficking, similarly increases Kv1.5 surface expression (Choi *et al.* 2005), perhaps by 'clogging' the internalization system as, meanwhile, newly synthesized channel is incorporated in the membrane. To test the possibility that Kv1.5 endocytosis was reduced by expression of the Rab4DN, we used immunocytochemistry to assay channel internalization in cells coexpressing the Rab4DN *versus* control. Consistent with this hypothesis, the dominant negative construct reduced the average number of vesicles harbouring surface-labelled, internalized Kv1.5 per cell by over 40%. Compare Kv1.5-HA associated fluorescence in the control and +Rab4DN panels of Fig. 10*A*. After 30 min internalization, control cells harboured an average of 45.1 ± 3.6 Kv1.5-positive vesicles per cell (20 cells, 1038 total vesicles) whereas cells expressing Rab4DN harboured only 26 ± 4.5 such vesicles (18 cells, 468 total vesicles; $P < 0.01$) (Fig. 10*B*). Unlike all control cells in all other experiments, two Rab4DN-expressing cells harboured zero Kv1.5-positive vesicles at this time point. Rab4DN is clearly interfering with Kv1.5 internalization.

Transferrin internalization, too, was reduced by Rab4DN expression (Fig. 10*C*). Total internalized transferrin after 5 min internalization time was reduced from an average of $12.1 \pm 0.7 \times 10^6$ fluorescence intensity

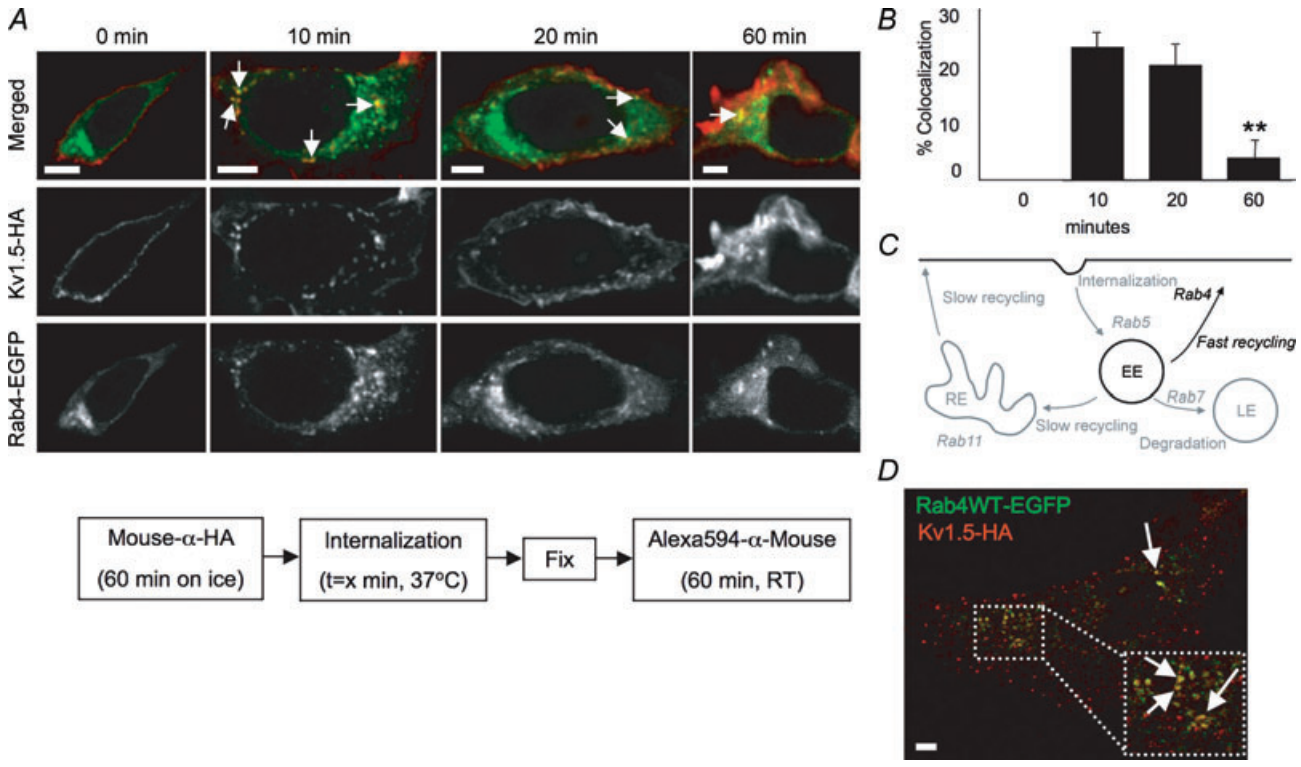

Figure 6. Kv1.5-HA colocalization with Rab4
A, time series of Kv1.5 colocalization with Rab4. Upper panels, merged Rab4-EGFP and Kv1.5-HA associated fluorescence at the indicated time points. The arrows highlight some of the vesicles in which Kv1.5 and Rab4 are seen to colocalize. Middle panels, Kv1.5-HA associated Alexa594 fluorescence alone. Only channels present at the beginning of the experiment are labelled. Lower panels, Rab4-EGFP fluorescence alone. The experimental protocol is outlined schematically below the images. Scale bar = 5 μm. *B*, percentage colocalization of Rab4 in Kv1.5-positive vesicles. Percentage colocalization was calculated from the fraction of Kv1.5 positive vesicles in the imaged cells that were found to exhibit tagged-Rab4 EGFP fluorescence also. *C*, Rab4-dependent steps highlighted in Rab-dependent pathway schematic diagram. EE, early endosome; RE, recycling endosome; LE, late endosome. *D*, Kv1.5-HA and Rab4-EGFP colocalize in H9c2 cells after 20 min internalization time. The arrows point to some of the vesicles in which colocalization is evident. $^{**}P < 0.01$, one-way ANOVA.

units per 1 μm thick optical slice in 16 control cells to $9.3 \pm 0.7 \times 10^6$ fluorescence intensity units in the same number of Rab4DN-expressing cells ($P < 0.05$, t test). Thus, block of Rab4 functioning may generally interfere with membrane protein internalization. Unlike Kv1.5, however, transferrin receptor surface expression was not significantly affected by the dominant negative. As assayed by transferrin surface binding in our imaging experiments, control cells averaged 4.5 ± 1.9 fluorescence intensity units per 1 μm optical slice at the cell surface whereas cells expressing the Rab4DN averaged 4.0 ± 1.5 fluorescence intensity units per slice at the cell surface.

We also tested whether the effect of the Rab4DN, too, converges on the dynein-dependent pathway that we previously identified, and found that indeed it does. We combined expression of the Rab4DN with p50 overexpression or with nocodazole. As shown in Fig. 11*A*, p50 overexpression increased Kv1.5 currents to the same extent as did Rab4DN expression; combined p50 and Rab4DN overexpression caused no further increase in the currents. Similarly, nocodazole treatment of control and Rab4DN-expressing cells showed no statistically significant additivity with Rab4DN in affecting Kv1.5 currents (Fig. 11*B*). Thus, similarly to that affected by the Rab5DN, the Rab4DN-induced increase in currents is related to the same Kv1.5-trafficking pathway in which dynein functions.

Internalized Kv1.5 associates with Rab11 only after prolonged periods

Cells possess more than one recycling pathway. In addition to the typically fast Rab4-dependent pathway, cells utilize also a slower, Rab11-dependent route to return membrane proteins to the cell surface (Fig. 12*C*). A fraction of transferrin receptor recycling occurs via this pathway (Sheff *et al.* 1999) and, as mentioned above, KCNQ1 recycling

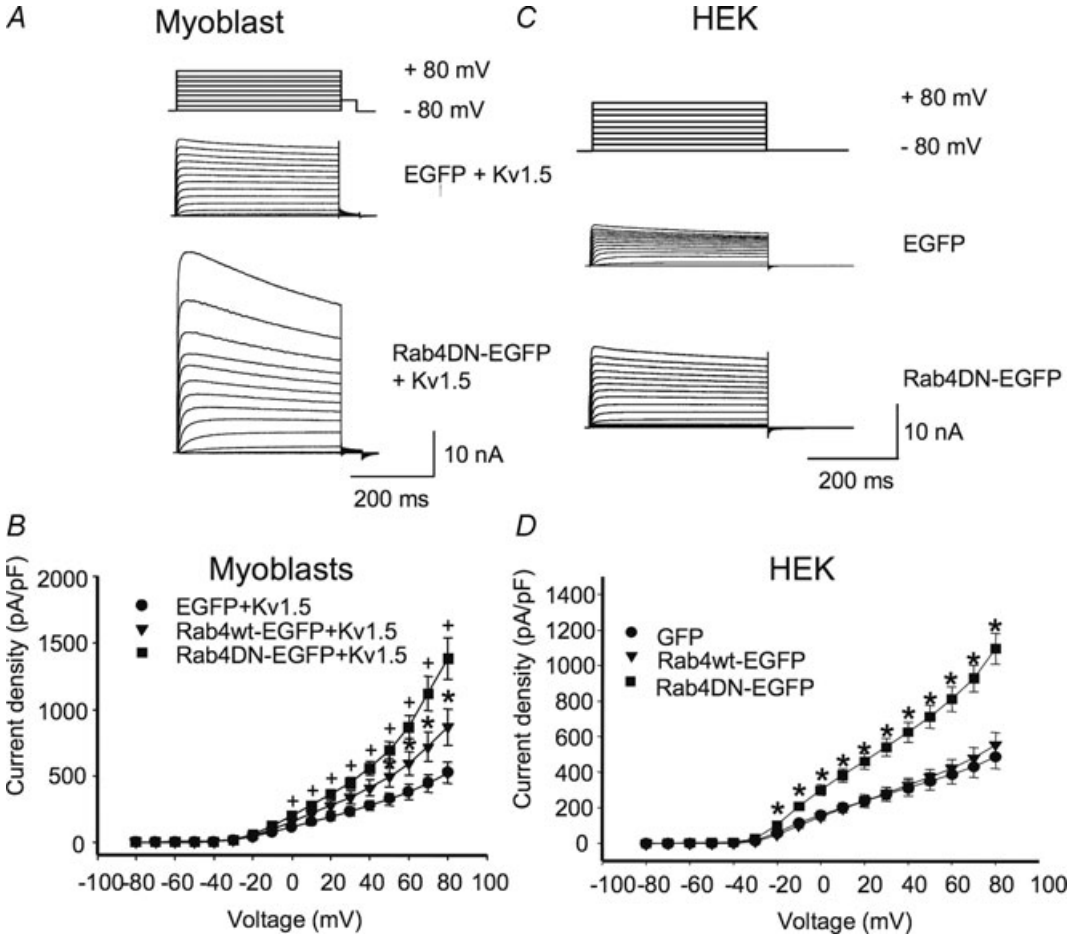

Figure 7. Rab4DN significantly increases Kv1.5 current density 24 h post-transfection
The electrophysiological protocols were as described in Fig. 4. Data are represented as means ± S.E.M. *A* and *C*, sample traces of control and Rab4DN-transfected H9c2 and HEK293 cells, respectively. The HEK293 line stably expresses Kv1.5; H9c2 cells were cotransfected with Kv1.5-mCherry. *B* and *D*, current–voltage plots for data recorded 24 h post-transfection for H9c2 and HEK293 cells, respectively. $+P < 0.01$, $^*P < 0.5$, one-way ANOVA.

is Rab11 dependent (Seebohm *et al.* 2007). When we assayed Kv1.5 trafficking through this Rab11-dependent pathway, our results differed substantially from those obtained for Rab5 and Rab4. No colocalization of Kv1.5 and Rab11 at all was seen within the first several hours post-labelling (Fig. 12*A*). By 24 h, however, colocalization of Rab11 with Kv1.5 was evident (highlighted by the arrows in Fig. 12*A*). Quantification of this colocalization showed that Rab11 was present in 25.2% of Kv1.5-HA positive vesicles (Fig. 12*B*). Thus, a fraction of the internalized channel does eventually traffic through Rab11-positive endosomes. This is similar to results reported for the β-adrenergic receptor, which also colocalizes with Rab11 only after prolonged periods of internalization (Moore *et al.* 2004).

Electrophysiological results were consistent with this finding. Unlike Rab5 and Rab4 dominant negatives, both of which induced significant increases in Kv1.5 currents

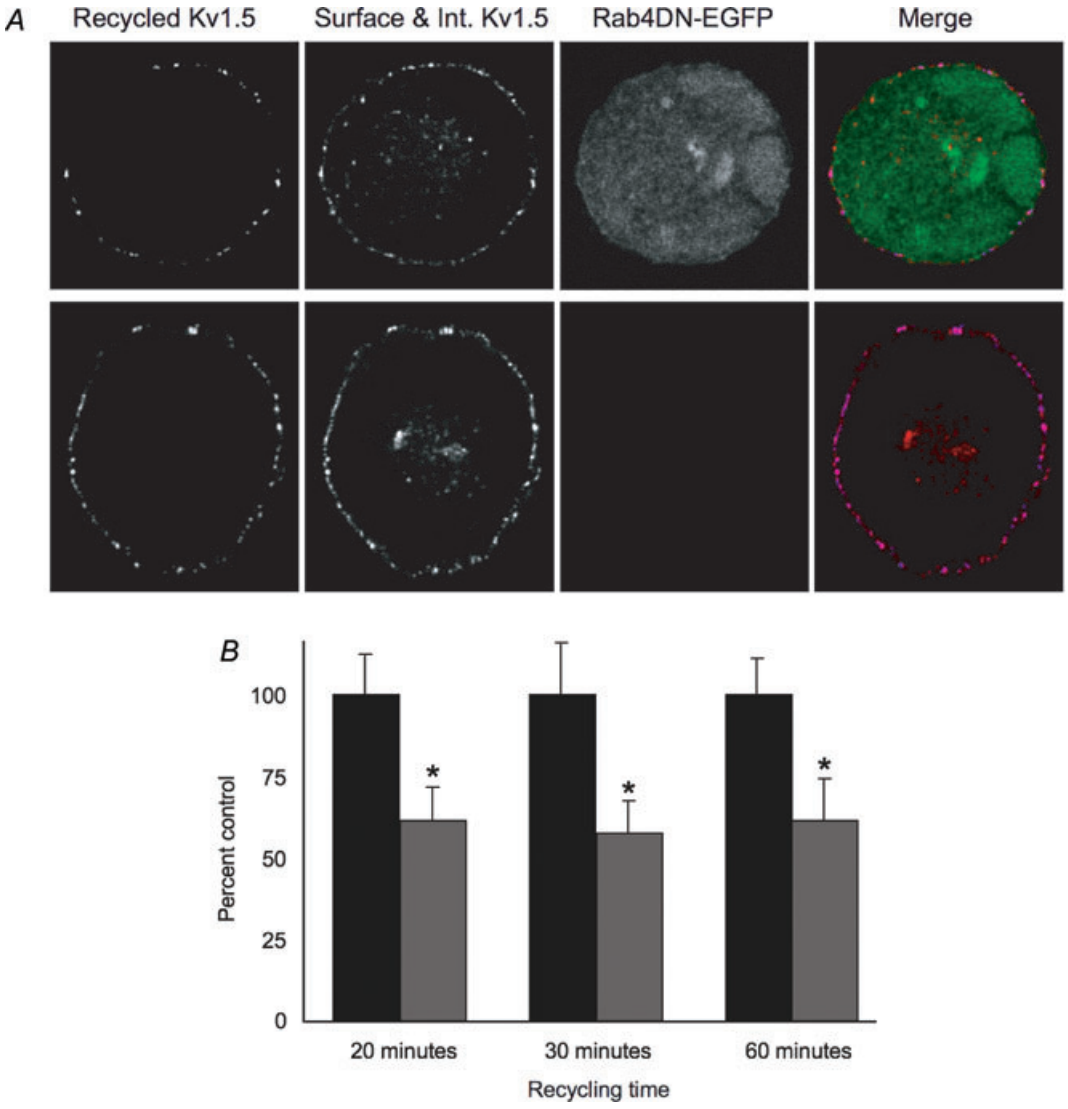

Figure 8. Co-expression of Rab4DN reduces Kv1.5 recycling
The recycling assay was as described for Fig. 2 with the exception that the experimental cells were transfected with pcDNA3-Rab4DN-EGFP and the recycled Kv1.5-HA was detected with Alexa Fluor 647 conjugated goat anti-mouse. *A*, representative images showing recycled Kv1.5-HA (blue, Alexa Fluor 647-conjugated) at the membrane and surface and internalized Kv1.5 (red, Rhodamine Red-X conjugated) in control, untransfected cells (upper panels) and in Rab4DN-EGFP expressing cells after 30 min recycling time (lower panels). Scale bar = 5 μm. *B*, relative pixel intensities of Alexa647 fluorescence (indicative of recycled Kv1.5) at the cell membrane under control conditions (dark bars) and when Rab4DN is coexpressed (light bars) at the indicated time points. Values are normalized to the control (untransfected) pixel intensities at each time point. Sample sizes for each time point are as follows: 20 min: Control $n = 15$, Rab4DN $n = 10$; 30 min: Control $n = 13$, Rab4DN $n = 11$; 60 min: Control $n = 6$, Rab4DN $n = 7$. $^*P < 0.05$, Student's *t* test.

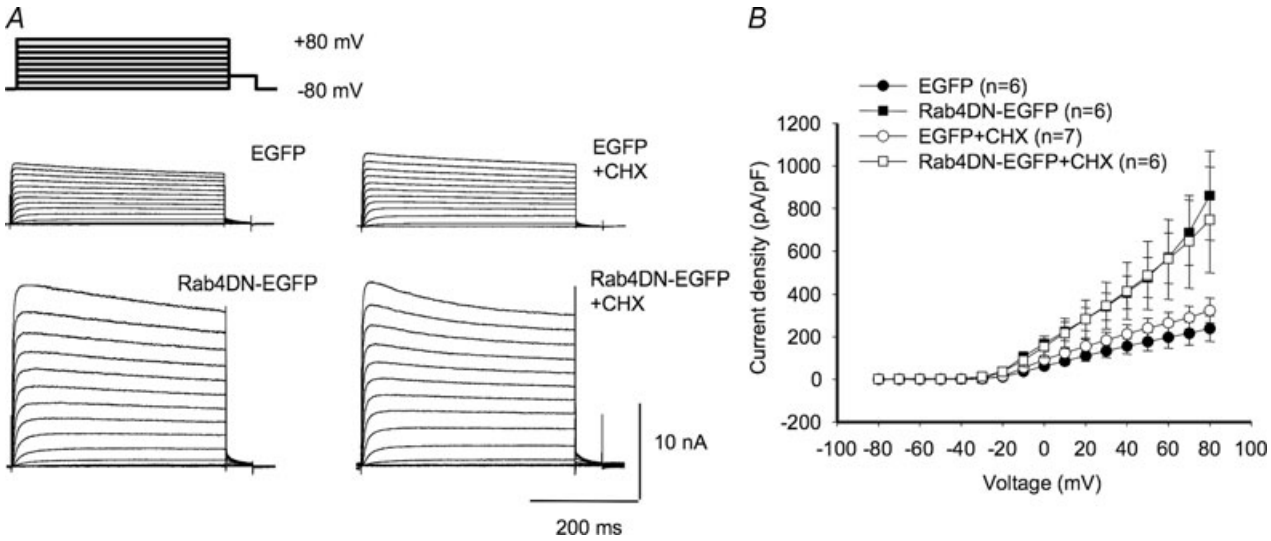

Figure 9. Cycloheximide does not affect Rab4DN-mediated increase in Kv1.5 expression
A, sample traces of control and Rab4DN-transfected HEK293 cells ± cycloheximide. The HEK293 line stably expresses Kv1.5. Cycloheximide-treated cells were treated with 100 μg/ml cycloheximide for 6 h immediately prior to electrophysiological recording. *B*, current–voltage plots for data recorded 36–48 h post-transfection.

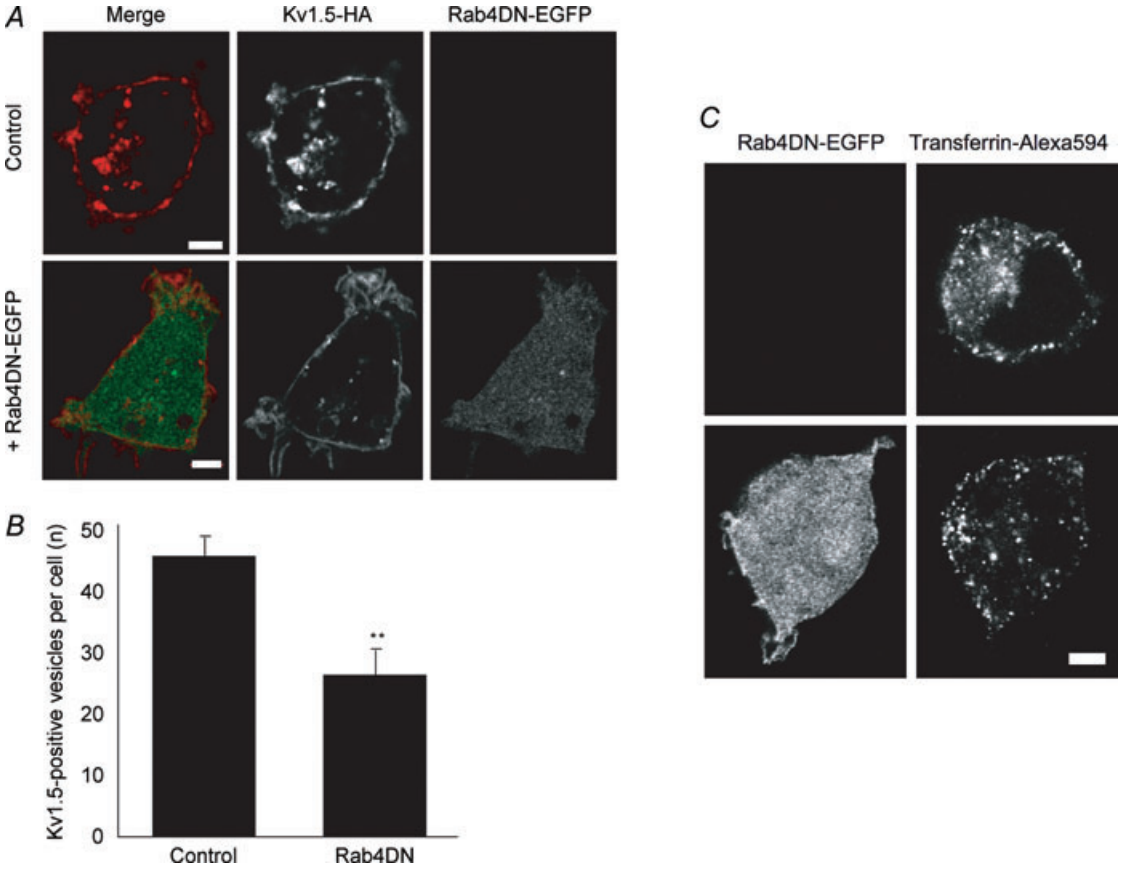

Figure 10. Co-expression of Rab4DN reduces Kv1.5 internalization
A, representative images showing internalized Kv1.5-HA positive vesicles in control (upper panels) and in Rab4DN-EGFP-transfected cells (lower panels). Kv1.5-HA is detected with Alexa Fluor 594 (red) and Rab5DN-EGFP is detected by EGFP (green) fluorescence. Only channels that were present at the cell surface at the beginning of the experiment are labelled. *B*, Number of Kv1.5-positive vesicles per cell under control conditions and when Rab4DN is coexpressed. $^{**}P < 0.01$, Student's *t* test. *C*, representative images showing internalized transferrin conjugated to Alexa Fluor 594 in control, untransfected cells (upper panels) and in Rab4DN-EGFP-transfected cells after 5 min internalization time. Scale bars = 5 μm.

within 24 h of transfection (Figs 4 and 7), the Rab11DN (Rab11 S25N) had no effect on Kv1.5 currents in this time frame (Fig. 13*B* and *E*). By 48 h post-transfection, however, the Rab11DN did induce increased Kv1.5 currents (Fig. 13*C* and *F*). In the H9c2 myoblasts this increase was quite robust (Fig. 13*A* and *C*). Current densities were increased to 1580 ± 205 pA pF^{-1} ($n = 10$) from the control 667 ± 101 pA pF^{-1} ($n = 10$). In HEK293 cells, the effect was less (Fig. 13*D* and *F*). Current densities averaged 1175 ± 99.8 pA pF^{-1} in Rab11DN-transfected cells ($n = 13$) *versus* 741 ± 117 pA pF^{-1} ($n = 13$) in control EGFP-transfected cells.

Co-expression of p50 with Rab11DN did not significantly increase Kv1.5 currents beyond those seen by transfection with either construct alone, 48 h after transfection (Fig. 13*G*). Interestingly, however, the combined effects of nocodazole plus Rab11DN were additive (Fig. 13*H*). Current densities were 925 ± 64.6 pA pF^{-1} ($n = 11$) in cells expressing Rab11DN and 828 ± 99.5 pA pF^{-1} ($n = 9$) in nocodazole-treated, EGFP-transfected cells. Combined, Rab11DN expression plus nocodazole increased currents to 1330 ± 194 pA pF^{-1} ($n = 10$) from the control level of 527.0 ± 61.0 pA pF^{-1} ($n = 13$). As Rab11 is involved also in trafficking of newly synthesized protein to the plasma membrane, it is possible that this additivity reflects an effect on that pathway as well as on the recycling of internalized channels. Treatment of cells for 6 h with 100 μg ml^{-1} cycloheximide, a protein synthesis inhibitor, immediately prior to patching had no influence on the increase in Kv1.5 expression, however (data not shown). Determination of the mechanism behind the Rab11DN-associated increase in Kv1.5 expression therefore will have to await further studies.

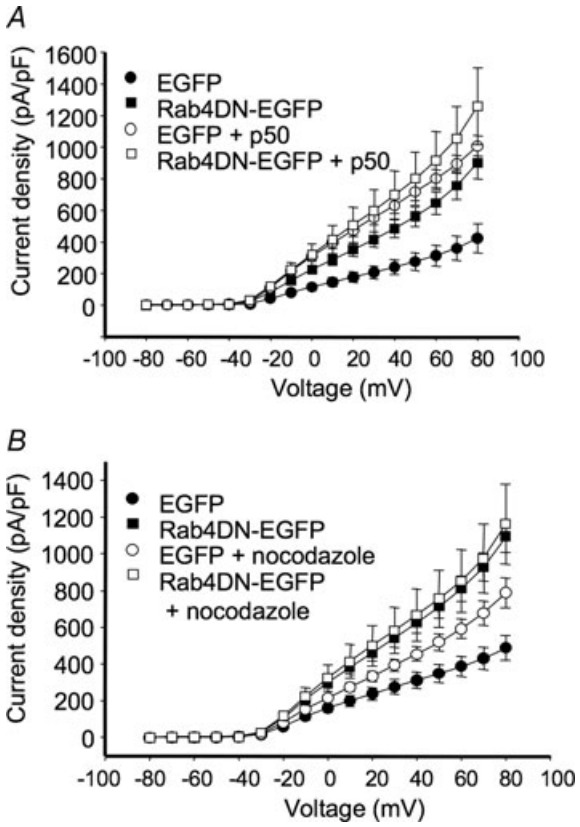

Figure 11. Effects of Rab4DN and interference with microtubule-dependent trafficking are not additive
Electrophysiological protocols were as described in Fig. 4. Data are represented as means ± S.E.M. *A*, effect of p50/dynamitin overexpression on Kv1.5 current density in control and Rab4DN-coexpressing HEK293 cells. Current recordings were performed 36–48 h post-transfection. *B*, current densities of control cells and Rab4DN-EGFP transfected cells with or without nocodazole treatment are plotted against voltage. Nocodazole-treated cells were incubated with 35 μM nocodazole for 6 h prior to electrophysiological recording.

Internalized Kv1.5 also traffics to the lysosomal degradation pathway

If all internalized Kv1.5 were to recycle to the plasma membrane, expression levels would inexorably rise as newly synthesized channel was also incorporated. With this in mind, we investigated whether internalized Kv1.5 traffics also to the degradation pathway as defined by Rab7 colocalization (Fig. 14*C*). A fraction of internalized transferrin receptor is shunted into this pathway (Sheff *et al.* 1999). As illustrated in Fig. 14*A*, Kv1.5 colocalization with Rab7 can first be detected after 30 min of internalization time (Fig. 14*A*), indicating that a fraction of internalized Kv1.5 is targeted for degradation. Although never as robust as with Rab5 or Rab4, some 9% of Kv1.5 positive vesicles also harbour Rab7 after 30 min internalization time. Colocalization peaks at 120 min, at which time 14% of vesicles containing Kv1.5 also contain Rab7 (Fig. 14*B*). Rab7 was found to similarly colocalize with Kv1.5 in H9c2 cells cotransfected with Kv1.5-HA and Rab7-EGFP (Fig. 14*D*).

Electrophysiological experiments confirmed a role for Rab7 in modulating Kv1.5 functional expression. Interestingly, in the myoblast cell line, the Rab7 dominant negative (Rab7 N125I; Rab7DN) had only modest effects on Kv1.5 currents but over-expression of wild-type Rab7 dramatically reduced Kv1.5 functional expression in the H9c2 myoblast cell line (Fig. 15*A* and *B*). Current densities in the wild-type Rab7-expressing myoblasts were reduced to 573 ± 96.3 pA pF^{-1} ($n = 7$) from the control 869 ± 136 pA pF^{-1} ($n = 8$). In contrast, in HEK293 cells, the dominant negative Rab7 dramatically increased Kv1.5 currents from the 629 ± 116 pA pF^{-1} ($n = 10$) seen in control cells to 1356 ± 333 pA pF^{-1} ($n = 9$), but the wild-type had no significant effect (Fig. 15*C* and *D*). Again, as for Rab4, perhaps Rab7 is limiting in the

myoblast cell line but plentiful in the HEK293 cells. Neither p50 overexpression nor nocodazole treatment was additive with the effects of the Rab7DN (Fig. 15*E* and *F*).

To confirm that Kv1.5 does indeed traffic to the lysosome, we tested for colocalization of internalized channel with a lysosomal marker, LAMP2. Surface Kv1.5HA was labelled with rabbit-anti-HA in HEK293 cells stably expressing Kv1.5. After 30 min incubation at 37°C, cells were fixed, permeabilized and stained for lysosomes using mouse-anti-LAMP2 (AC17) monoclonal antibody and appropriate secondary antibodies. Figure 16 includes representative images showing colocalization after 30 min internalization time of Kv1.5-HA and LAMP2 in HEK293. Thus, after internalization, a fraction of Kv1.5 traffics to the lysosome for degradation.

Finally, we tested whether blockade of lysosomal function would prevent the reduction in Kv1.5 expression associated with Rab7 wild-type expression in H9c2 cells. To accomplish this, cells were incubated with 50 mM ammonium chloride for 6 h prior to electrophysiological experiments. Ammonium chloride accumulates in the lysosome, neutralizing the pH and preventing degradation of proteins present in the organelle. As illustrated in Fig. 17, this treatment completely blocked any reduction in Kv1.5 expression by the Rab7 wild-type in these cells. Co-expression of Rab7 wild-type with Kv1.5 reduced expression from a control 435.5 ± 81.4 pA pF^{-1} to 246.1 ± 47.1 pA pF^{-1} in the absence of ammonium chloride (Fig. 17*B*). In the presence of the lysosomal inhibitor, however, Rab7 wild-type had no statistically significant effect on Kv1.5 functional expression. Current densities were 545.2 ± 99.3 pA pF^{-1} in ammonium chloride-treated control cells and 713.3 ± 147.2 pA pF^{-1} in similarly treated cells coexpressing Rab7. Thus, the lysosomal degradation pathway plays an important role in the regulation of Kv1.5 surface expression.

Discussion

We have demonstrated the involvement of four Rab-GTPases, Rab5, Rab4, Rab11 and Rab7, in the trafficking and recycling of surface-expressed Kv1.5 following internalization from the plasma membrane. Internalized Kv1.5 colocalizes rapidly with Rab5 and Rab4, more slowly with Rab7 and, much later, with Rab11, indicating that a significant fraction of this population recycles to the plasma membrane in short

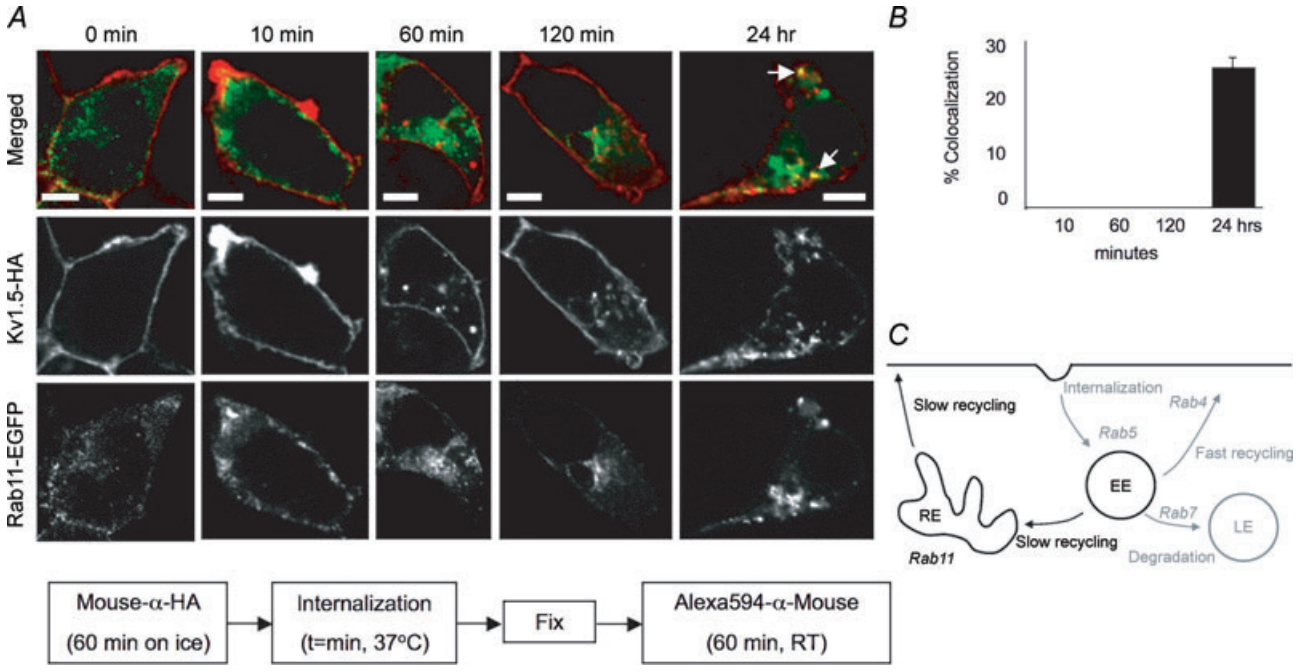

Figure 12. Kv1.5 colocalizes with Rab11 only after prolonged internalization times
A, time series of Kv1.5 colocalization with Rab11. Upper panels, merged Rab11-EGFP and Kv1.5-HA associated fluorescence at the indicated time points. The arrows highlight some of the vesicles in which Kv1.5 (red) and Rab11 (green) are seen to colocalize (yellow). Middle panels, Kv1.5-HA associated Alexa Fluor 594 fluorescence alone. Only channels that were present at the cell surface at the beginning of the experiment are labelled. Lower panels, Rab11-EGFP fluorescence alone. The schematic below outlines the protocol employed in these experiments. Scale bar = 5 μm. *B*, percentage colocalization of Rab11 in Kv1.5-positive vesicles. *C*, Rab11-dependent steps highlighted in Rab-dependent pathway schematic diagram. EE, early endosome; RE, recycling endosome; LE, late endosome.

order after endocytosis, and another fraction is targeted for degradation. Co-expression of dominant negative Rab mutants confirmed the roles of these GTPases in Kv1.5 trafficking. When assayed electrophysiologically, both Rab5 and Rab4 dominant negatives roughly tripled Kv1.5 currents 24–48 h post-transfection. The Rab11 dominant negative also increased Kv1.5 currents but this increase was seen only at 48 h post-transfection. Both Rab5 and Rab4 dominant negatives reduced the number of Kv1.5 positive vesicles, suggesting that the increased currents measured resulted from reduced endocytosis of the channel.

Our results have similarities to those reported by Seebohm *et al.* (2007) for KCNQ1/KCNE1. They found that KCNQ1 internalization is Rab5 dependent and that recycling in response to activation of the SGK1 kinase depends on Rab11. McEwen *et al.* (2007), also, have recently reported that Kv1.5 recycles to the plasma membrane. Using purely immunocytochemical techniques, these workers tested the involvement of Rab4, Rab5 and Rab11 in Kv1.5 trafficking. Like us, they demonstrated involvement of Rab4 and Rab11 in this process, but, unlike us, did not detect Rab5 involvement. Also, unlike our results, they found that both Rab4 and Rab11 reduced Kv1.5 surface expression. The differences between the results of McEwen *et al.* and those reported here may be related to substantially different experimental techniques. McEwen *et al.* relied entirely on immunocytochemistry of transiently transfected cells in generating their results, measuring the ratio of surface to internal staining in assessing changes in Kv1.5 surface expression.

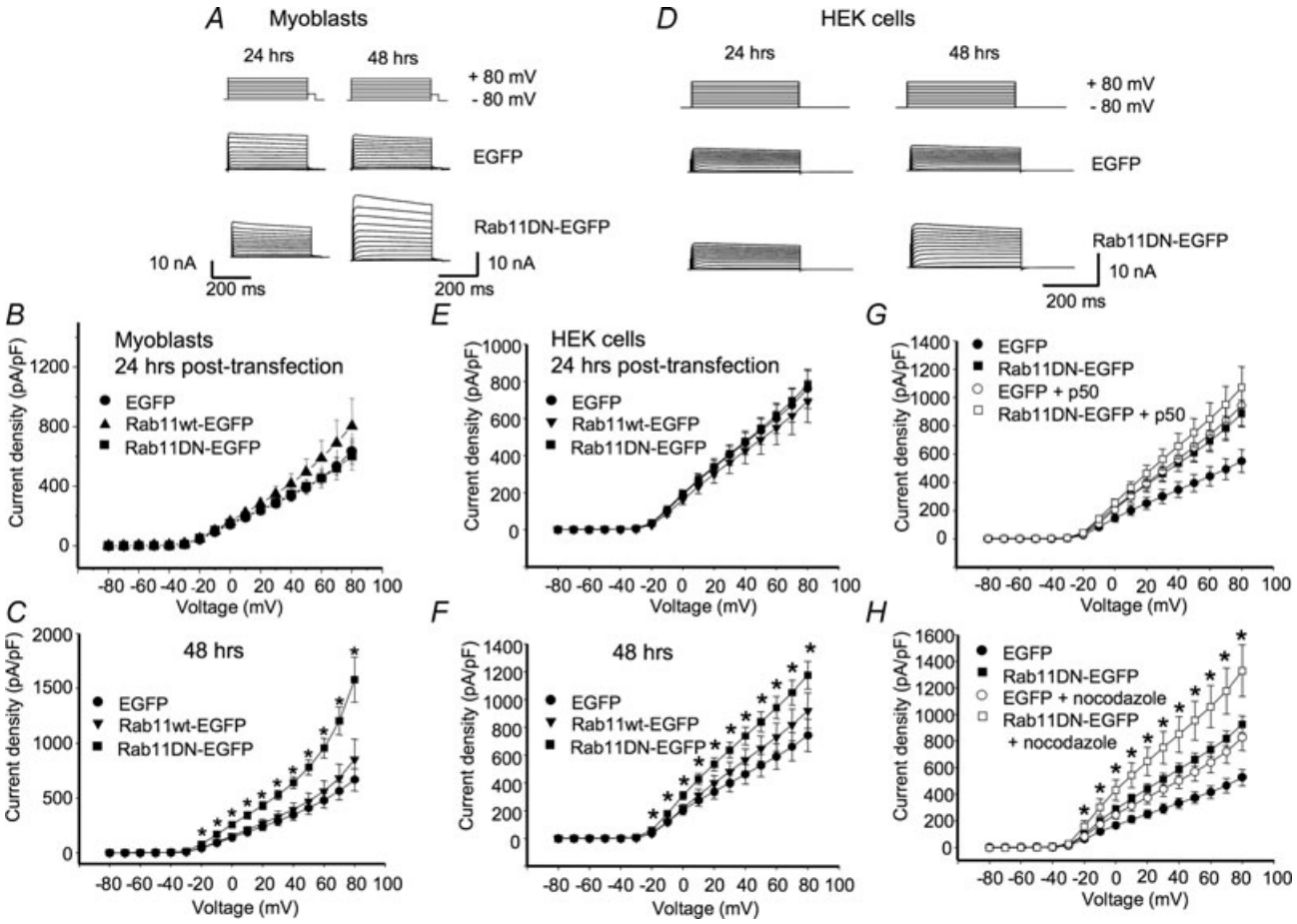

Figure 13. Rab11DN affects Kv1.5 currents only late after transfection
The electrophysiological protocols were as described in Fig. 4. Data are represented as means ± S.E.M. *A* and *D*, sample traces for data recorded 24 and 48 h post-transfection in H9c2 cells and HEK293 cells, respectively. The HEK293 line stably expresses Kv1.5; H9c2 cells were cotransfected with Kv1.5-mCherry. *B* and *E*, current density plots for data recorded 24 h post-transfection from H9c2 and HEK293 cells, respectively. *C* and *F*, current density plots recorded 48 h post-transfection from H9c2 and HEK293 cells, respectively. *G*, effect of p50/dynamitin overexpression on Kv1.5 current density in HEK293 cells. Current recordings were performed 48 h post-transfection. *H*, current densities, 48 h post-transfection, of control cells and Rab11DN-EGFP transfected HEK293 cells with or without nocodazole treatment are plotted against voltage. Nocodazole-treated cells were incubated with 35 μM nocodazole for 6 h prior to electrophysiological recording. $^*P < 0.05$, one-way ANOVA.

In our hands, this is an unreliable approach; variation in expression from transfection to transfection and from cell to cell has substantial effects on the surface to internal staining ratio. Electrophysiological measurements are likely to be much better barometers of actual Kv1.5 surface expression. Also, the use of intact secondary antibodies to detect externally GFP tagged Kv1.5 may have affected Kv1.5 trafficking in the system used by McEwen *et al.* Intact antibodies can crosslink adjacent channels and substantial crosslinking of channels by the antibodies may well affect channel internalization. To avoid crosslinking, we used only the Fab fragments as secondary antibodies for all live cell experiments. In any case, our results are in agreement with theirs to the extent that we have both demonstrated the involvement of Rab4 and Rab11 in Kv1.5 trafficking.

Internalization and early trafficking are dependent upon Rab5

In addition to its role in early endosome fusion and maturation (Simonsen *et al.* 1998; Christoforidis *et al.* 1999), Rab5 is important to clathrin-mediated endocytosis (Bucci *et al.* 1992). Thus, the simplest interpretation of the increased Kv1.5 currents detected following transfection with Rab5DN is that the dominant negative blocks endocytosis of the channel. This interpretation is consistent with the previously demonstrated effect of a dynamin inhibitory peptide on Kv1.5 functional expression (Choi *et al.* 2005). Less likely, Kv1.5 may internalize in a clathrin-independent manner as suggested by Folco *et al.* (2004). Under this alternative scenario, Rab5DN might cause a failure of endocytosis as

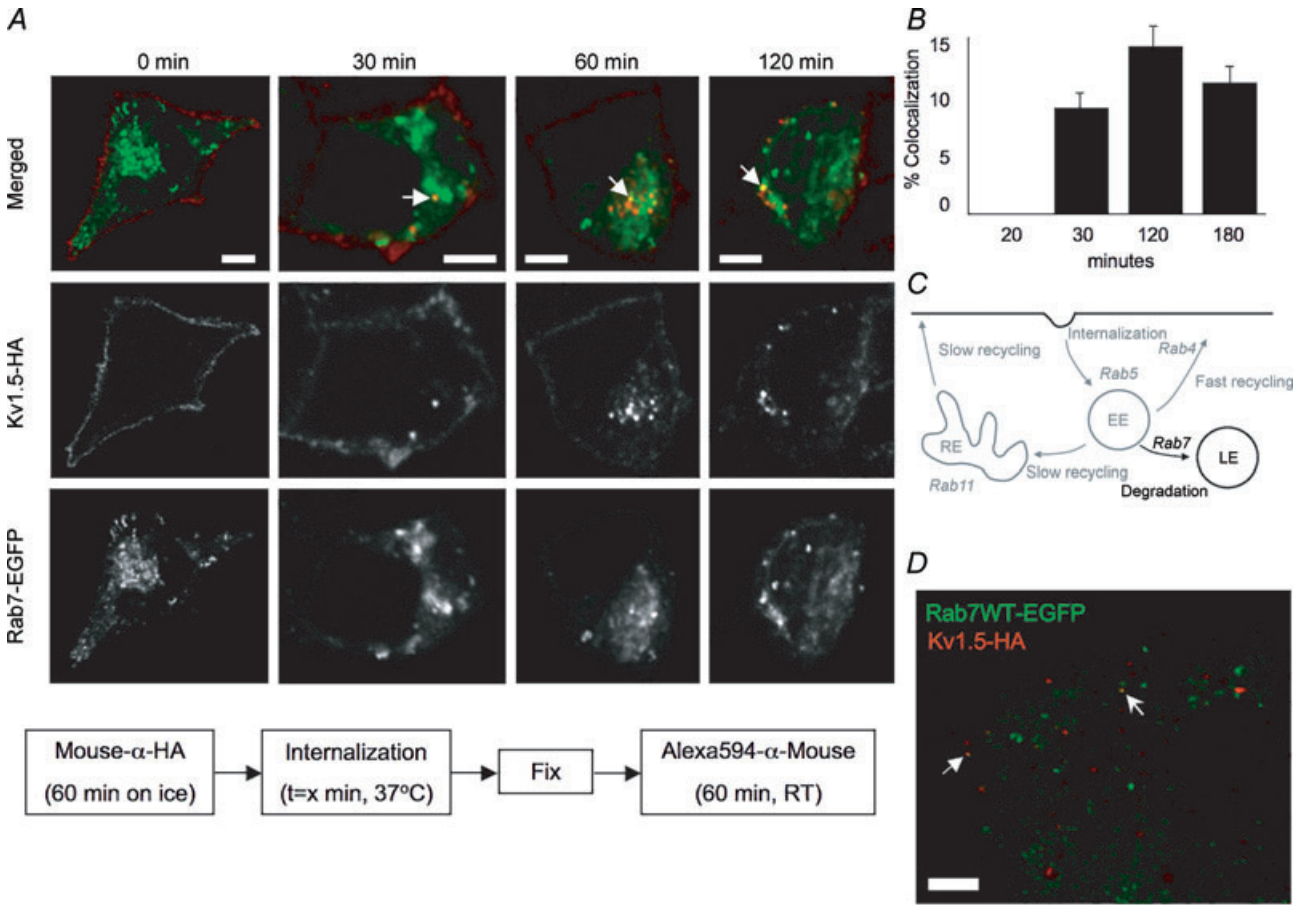

Figure 14. Kv1.5 colocalizes with Rab7 within 1 h of internalization
A, time series of internalized Kv1.5 colocalization with Rab7. The schematic diagram below outlines the protocol employed in these experiments. Upper panels, merged Rab7-EGFP and Kv1.5HA associated fluorescence at the indicated time points. The arrows highlight some of the vesicles in which Kv1.5 (red) and Rab7 (green) are seen to colocalize (yellow). Middle panels, Kv1.5-HA associated Alexa Fluor 594 fluorescence alone. Only channels that were present at the cell surface at the beginning of the experiment are labelled. Lower panels, Rab7-EGFP fluorescence alone. Scale bar = 5 μm. *B*, quantification of Rab7 colocalization in Kv1.5-positive vesicles. Percentage colocalization was calculated from the fraction of Kv1.5 positive vesicles in the imaged cells that were found to exhibit also tagged-Rab7 EGFP fluorescence. *C*, Rab7-dependent steps highlighted in Rab-dependent pathway schematic diagram. EE, early endosome; RE, recycling endosome; LE, late endosome. *D*, Kv1.5-HA and Rab7-EGFP colocalize in H9c2 cells after 20 min internalization time.

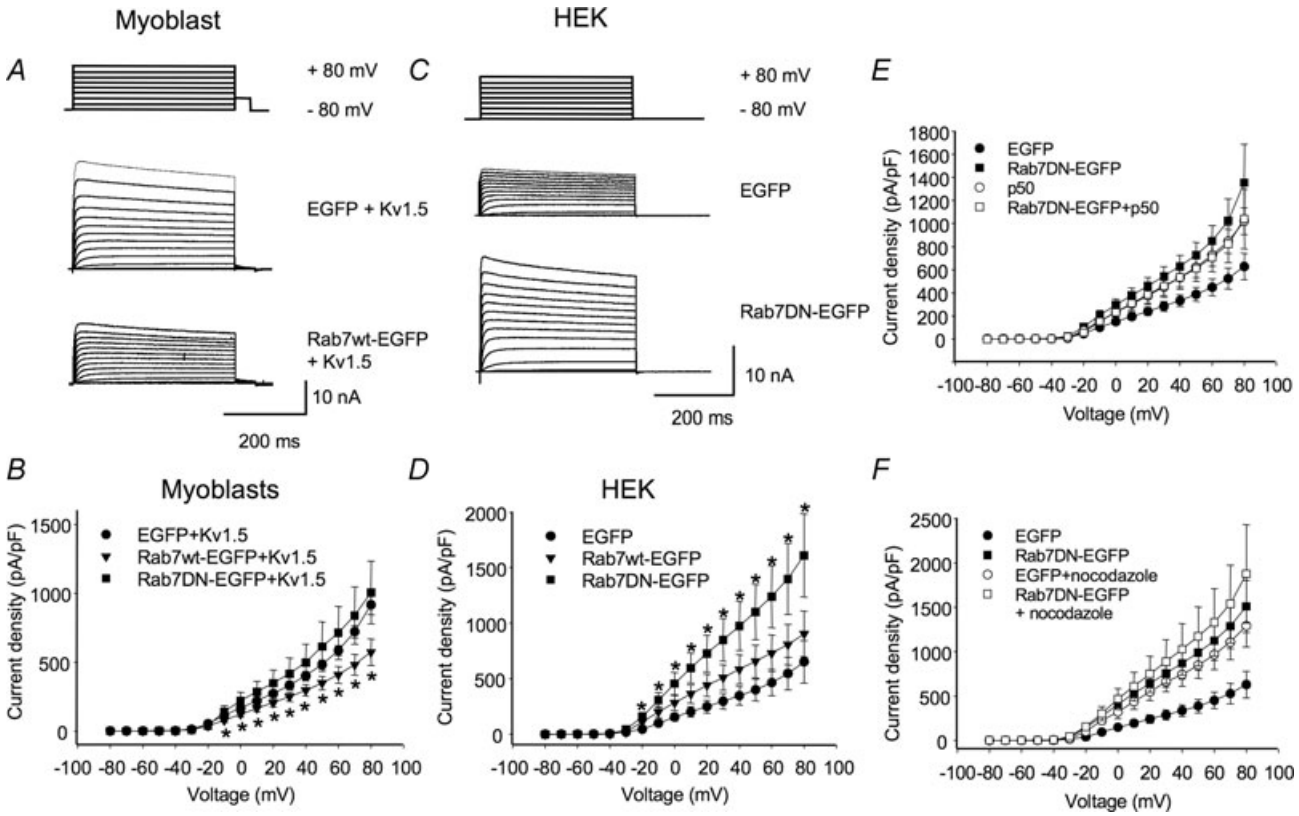

Figure 15. Rab7 wild-type and dominant negatives affect Kv1.5 functional expression
Electrophysiological protocols were as described in Fig. 4. Data are represented as means ± S.E.M. *A* and *C*, sample traces for data recorded 24 h post-transfection in H9c2 cells and HEK293 cells, respectively. The HEK293 line stably expresses Kv1.5; H9c2 cells were cotransfected with Kv1.5-mCherry. *B* and *D*, current density plots for data recorded 24 h post-transfection from H9c2 and HEK293 cells, respectively. *E*, effect of p50/dynamitin overexpression Kv1.5 current density in HEK293 cells coexpressing Rab7 EGFP fusions. Current recordings were performed 36–48 h post-transfection. *F*, current densities of control cells and Rab7 wild-type and Rab7DN-EGFP transfected HEK293 cells with or without nocodazole treatment are plotted against voltage. Nocodazole-treated cells were incubated with 35 μM nocodazole for 6 h prior to electrophysiological recording. $^*P < 0.05$, one-way ANOVA.

internalized vesicles accumulate or, perhaps, cause the rapid recycling of immature vesicles to the plasma membrane. Whether Kv1.5 is indeed internalized via caveolae is controversial. Unlike Folco *et al.* (2004), we were unable in our laboratory to detect the channel in these structures (Eldstrom *et al.* 2006). Whatever the case, that the effects of the Rab5 dominant negative and those of p50/dynamitin and nocodazole on Kv1.5 currents are comparable and non-additive strongly suggests that all are affecting the same trafficking pathway.

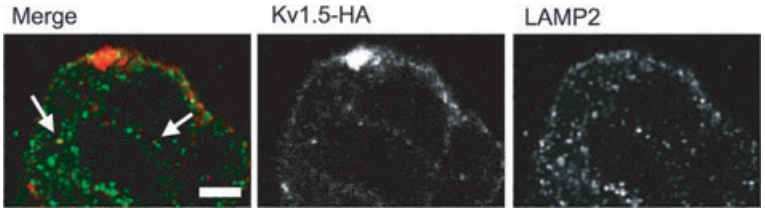

Figure 16. Kv1.5 colocalizes with LAMP2, a lysosomal marker
Representative images showing internalized Kv1.5-HA (Alexa Fluor 594, red) and LAMP2 (Alexa Fluor 488, green) staining in HEK293 cells stably expressing Kv1.5-HA. Only channels that were present at the cell surface at the beginning of the experiment are labelled. The arrows highlight some of the vesicles in which Kv1.5 (red) and LAMP2 (green) are seen to colocalize (yellow). Scale bar = 5 μm.

Rab4 very probably mediates rapid Kv1.5 recycling to the plasma membrane

Colocalization of Kv1.5 with Rab4 begins on a time scale just slightly longer than seen with Rab5. Rab4 is known to be involved with the rapid recycling of other membrane proteins such as the transferrin receptor (Sheff *et al.* 2002) and the amiloride-sensitive sodium channel, ENaC (Saxena *et al.* 2006). Thus, it is likely that a substantial portion of endocytosed Kv1.5 similarly recycles to the plasma membrane in a Rab4-dependent manner. Reportedly, some 70% of internalized transferrin receptor recycles through this pathway returning to the plasma membrane within 10 min of endocytosis (Sheff *et al.* 1999). That the majority of Kv1.5-positive vesicles are quite immobile is consistent with this hypothesis (see Fig. 1*B*). Highly mobile or 'dynamic' early endosomes have been associated with the degradation pathway whereas static early endosomes are reportedly targeted for rapid recycling (Lakadamyali *et al.* 2006). The transferrin receptor evidently segregates randomly into static and dynamic populations of early endosomes and, because static endosomes are more common, the internalized receptor is more often recycled than degraded. It will be interesting to learn whether Kv1.5 segregation in endosomes is similarly random or is somehow actively regulated.

It is interesting also that Kv1.5 surface expression was increased and channel internalization reduced when a Rab4 dominant negative was coexpressed in our system. As demonstrated by the fact that cycloheximide had no effect on this increase in surface expression, it is highly unlikely that incorporation of newly synthesized channel is behind this increase. Perhaps, because they are unable to recycle to the plasma membrane, early endosomes instead accumulate, preventing Rab5 cycling out of these endosomes. This could create a shortage of Rab5 for clathrin-mediated endocytosis, thereby slowing channel internalization. Consistent with this hypothesis, expression of a dominant negative Rab4 analogue in *Dictyostelium discoideum* has also been shown to reduce the rate of endocytosis in that organism (Bush *et al.* 1996). There is some evidence that Rab4 may be involved also in degradative trafficking to the lysosome (McCaffrey *et al.* 2001; Cormont *et al.* 2003). Thus, an alternative, if less likely, explanation for the increased current densities invoked by the Rab4DN may be that channel degradation is impaired and Kv1.5 recycling through the Rab11 pathway is somehow facilitated. Of course, a failure of early endosomes to mature and target to the degradative pathway could interfere with endocytosis in the same manner as discussed above.

The role of Rab11 in trafficking of internalized Kv1.5 is limited

Whereas Rab4 associates with early endosomes (Grosshans *et al.* 2006), Rab11 is found in pericentriolar recycling endosomes, a population of endosomes through which

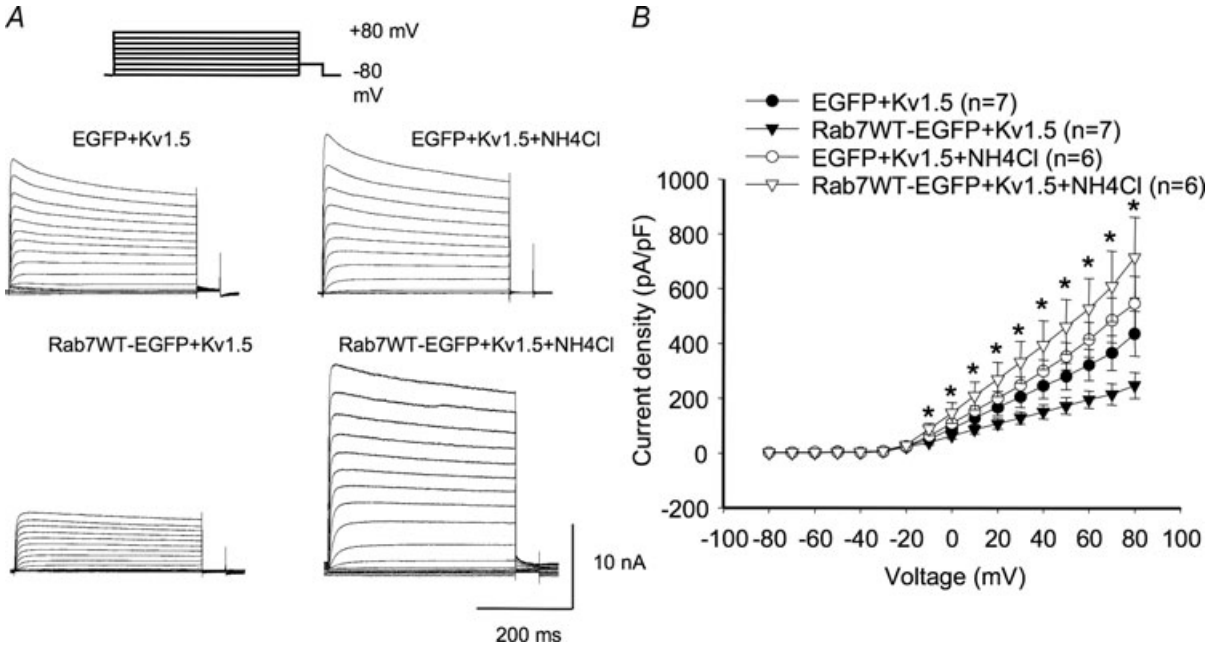

Figure 17. Ammonium chloride prevents Rab7-associated decrease in H9c2 cell Kv1.5 expression
A, sample traces of control and Rab4DN-transfected H9c2 cells ± ammonium chloride. H9c2 cells were treated with 50 mM ammonium chloride for 6 h immediately prior to electrophysiological recording. *B*, current–voltage plots for data recorded 36–48 h post-transfection. $^*P < 0.05$, comparing Rab7 wild-type over-expressing cells ± ammonium chloride.

many membrane proteins recycle (Ullrich *et al.* 1996). Rab11 is found also in the *trans*-Golgi network and post-Golgi vesicles where it is involved in the trafficking of many newly synthesized proteins from that organelle to the cell surface (Grosshans *et al.* 2006). We found that Kv1.5 also associates with Rab11 in probable recycling endosomes but that it does so only after prolonged periods of internalization. Like the Rab5 and Rab4 dominant negatives, the Rab11DN caused an increase in Kv1.5 functional expression, but unlike Rab5DN and Rab4DN, this increase was detectable only at 48 h and not at 24 h post-transfection (Fig. 12). Perhaps Kv1.5 is marked for transport to Rab11-positive vesicles only after multiple Rab4-dependent recycling events.

Interestingly, the effects of the Rab11DN and the microtubule depolymerizing agent, nocodazole, were additive. Whereas with Rab4DN nocodazole cotreatment caused no further increase in Kv1.5 surface expression, with the Rab11DN nocodazole essentially doubled the effect. As the effects of p50 over-expression were not additive with the dominant negative, it is likely that microtubule depolymerization combined with Rab11DN expression has affected Kv1.5 trafficking via a pathway separate from that involving Rab5 and Rab4. Perhaps nocodazole, in the presence of the Rab11DN, has somehow accelerated the forward trafficking of newly synthesized Kv1.5 from the Golgi to the cell surface. That cycloheximide, a potent inhibitor of protein synthesis, did not inhibit the Rab11DN-associated increase in Kv1.5 expression, however, speaks against this possibility. Conceivably instead, when Rab11 function is impaired, perinuclear recycling endosomes somehow more freely diffuse to the plasma membrane. Alternatively, Kv1.5 in vesicles normally destined for transformation into Rab11-positive endosomes may be freed by the nocodazole for more rapid trafficking back to the surface when formation of these Rab11-associated endosomes is inhibited.

Kv1.5 also traffics into the lysosomal degradation pathway

Kv1.5 associates quite quickly with Rab7, indicating that a significant fraction of internalized channel is targeted for degradation. Colocalization is apparent within 30 min of surface channel labelling but this colocalization is limited and remains so through at least 3 h of channel internalization/trafficking. As demonstrated by colocalization with LAMP2, a fraction of Kv1.5 makes it beyond the late endosome and on to the lysosome within 30 min of channel internalization. Interestingly, coexpression of the Rab7DN increased Kv1.5 currents in HEK293 cells stably expressing the channel but had no significant effect on Kv1.5 currents when the two proteins were coexpressed in H9c2 cells. Over-expression of the wild-type Rab7 protein, on the other hand, substantially reduced Kv1.5 functional expression in the H9c2 cells but had no significant effect on channel expression in the HEK293 line. The simplest explanation for these findings is that Rab7 is limiting in the myoblast cell line but present in excess in the HEK293 cells. Thus, increased expression of the wild-type in the myoblast line allows a larger fraction of the internalized channel to be shunted to the degradation pathway. This hypothesis is supported by our finding that inhibition of lysosomal function by ammonium chloride prevents the decrease in channel expression associated with wild-type Rab7 overexpression in the H9c2 cells. Similarly, expression of the dominant negative in the myoblast line has little effect because only a small fraction of the channel would normally traffic through Rab7-positive endosomes. In the HEK293 cells, where a significant fraction of internalized Kv1.5 is normally targeted to this degradation pathway, the dominant negative prevents this trafficking and the channel is instead recycled to the plasma membrane and/or endocytosis is indirectly slowed.

In summary, we have implicated four prototypical Rab GTPases in the trafficking of Kv1.5 internalized from the plasma membrane. The expression of proteins that are internalized and recycle to the plasma membrane can be more finely regulated both temporally and spatially than can proteins more solidly anchored at the cell surface (Mostov *et al.* 1992). It is likely that the internalization and recycling/degradation of Kv1.5 allows the cell to regulate the expression level of this channel in response to physiological signals. It will be interesting to investigate the means by which this internalization and transport are regulated in both health and disease. Of particular interest may be the regulation of Kv1.5 trafficking in patients with chronic atrial fibrillation where Kv1.5 functional expression is reduced (Van Wagoner *et al.* 1997) as well as in other types of cardiac remodelling.

References

Bucci C, Parton RG, Mather IH, Stunnenberg H, Simons K, Hoflack B & Zerial M (1992). The small GTPase Rab5 functions as a regulatory factor in the early endocytic pathway. *Cell* **70**, 715–728.

Burkhardt JK, Echeverri CJ, Nilsson T & Vallee RB (1997). Overexpression of the dynamitin (p50) subunit of the dynactin complex disrupts dynein-dependent maintenance of membrane organelle distribution. *J Cell Biol* **139**, 469–484.

Bush J, Temesvari L, Rodriguez-Paris J, Buczynski G & Cardelli J (1996). A role for a Rab4-like GTPase in endocytosis and in regulation of contractile vacuole structure and function in *Dictyostelium discoideum*. *Mol Biol Cell* **7**, 1623–1638.

Choi WS, Khurana A, Mathur R, Viswanathan V, Steele DF & Fedida D (2005). Kv1.5 surface expression is modulated by retrograde trafficking of newly endocytosed channels by the dynein motor. *Circ Res* **97**, 363–371.

Christoforidis S, McBride HM, Burgoyne RD & Zerial M (1999). The Rab5 effector EEA1 is a core component of endosome docking. *Nature* **397**, 621–625.

Cormont M, Meton I, Mari M, Monzo P, Keslair F, Gaskin C, Mcgraw TE & Marchand-Brustel Y (2003). CD2AP/CMS regulates endosome morphology and traffic to the degradative pathway through its interaction with Rab4 and c-Cbl. *Traffic* **4**, 97–112.

Echeverri CJ, Paschal BM, Vaughan KT & Vallee RB (1996). Molecular characterization of the 50-kD subunit of dynactin reveals function for the complex in chromosome alignment and spindle organization during mitosis. *J Cell Biol* **132**, 617–633.

Eldstrom J, Van Wagoner DR, Moore ED & Fedida D (2006). Localization of Kv1.5 channels in rat and canine myocyte sarcolemma. *FEBS Lett* **580**, 6039–6046.

Fadool DA, Holmes TC, Berman K, Dagan D & Levitan IB (1997). Tyrosine phosphorylation modulates current amplitude and kinetics of a neuronal voltage-gated potassium channel. *J Neurophysiol* **78**, 1563–1573.

Filipeanu CM, Zhou F, Lam ML, Kerut KE, Claycomb WC & Wu GY (2006). Enhancement of the recycling and activation of β-adrenergic receptor by Rab4 GTPase in cardiac myocytes. *J Biol Chem* **281**, 11097–11103.

Folco EJ, Liu GX & Koren G (2004). Caveolin-3 and SAP97 form a scaffolding protein complex that regulates the voltage-gated potassium channel Kv1.5. *Am J Physiol Heart Circ Physiol* **287**, H681–H690.

Grosshans BL, Ortiz D & Novick P (2006). Rabs and their effectors: Achieving specificity in membrane traffic. *Proc Natl Acad Sci U S A* **103**, 11821–11827.

Holmes TC, Fadool DA, Ren R & Levitan IB (1996). Association of Src tyrosine kinase with a human potassium channel mediated by SH3 domain. *Science* **274**, 2089–2091.

Kessler A, Tomas E, Immler D, Meyer HE, Zorzano A & Eckel J (2000). Rab11 is associated with GLUT4-containing vesicles and redistributes in response to insulin. *Diabetologia* **43**, 1518–1527.

Lakadamyali M, Rust MJ & Zhuang XW (2006). Ligands for clathrin-mediated endocytosis are differentially sorted into distinct populations of early endosomes. *Cell* **124**, 997–1009.

Liu LJ & Askari A (2006). β-Subunit of cardiac Na^+-K^+-ATPase dictates the concentration of the functional enzyme in caveolae. *Am J Physiol Cell Physiol* **291**, C569–C578.

McCaffrey MW, Bielli A, Cantalupo G, Mora S, Roberti V, Santillo M, Drummond F & Bucci C (2001). Rab4 affects both recycling and degradative endosomal trafficking. *FEBS Lett* **495**, 21–30.

McEwen DP, Schumacher SM, Li Q, Benson MD, Iniguez-Lluhi JA, Van Genderen KM & Martens JR (2007). Rab-GTPase-dependent endocytic recycling of KV1.5 *in atrial myocytes. J Biol Chem* **282**, 29612–29620.

Moore RH, Millman EE, Alpizar-Foster E, Dai WP & Knoll BJ (2004). Rab11 regulates the recycling and lysosome targeting of β_2-adrenergic receptors. *J Cell Sci* **117**, 3107–3117.

Mostov K, Apodaca G, Aroeti B & Okamoto C (1992). Plasma-membrane protein sorting in polarized epithelial cells. *J Cell Biol* **116**, 577–583.

Nabi IR, Lebivic A, Fambrough D & Rodriguezboulan E (1991). An endogenous Mdck lysosomal membrane glycoprotein is targeted basolaterally before delivery to lysosomes. *J Cell Biol* **115**, 1573–1584.

Nesti E, Everill B & Morielli AD (2004). Endocytosis as a mechanism for tyrosine kinase dependent suppression of a voltage gated potassium channel. *Mol Biol Cell* **15**, 4073–4088.

Odley A, Hahn HS, Lynch RA, Marreez Y, Osinska H, Robbins J & Dorn GW (2004). Regulation of cardiac contractility by Rab4-modulated β_2-adrenergic receptor recycling. *Proc Natl Acad Sci U S A* **101**, 7082–7087.

Pfeffer SR (2001). Rab GTPases: specifying and deciphering organelle identity and function. *Trends Cell Biol* **11**, 487–491.

Saxena SK, Singh M, Shibata H, Kaur S & George C (2006). Rab4 GTP/GDP modulates amiloride-sensitive sodium channel (ENaC) function in colonic epithelia. *Biochem Biophys Res Comm* **340**, 726–733.

Seebohm G, Strutz-Seebohm N, Birkin R, Dell G, Bucci C, Spinosa MR, Baltaev R, Mack AF, Korniychuk G, Choudhury A, Marks D, Pagano RE, Attali B, Pfeufer A, Kass RS, Sanguinetti MC, Tavare JM & Lang F (2007). Regulation of endocytic recycling of KCNQ1/KCNE1 potassium channels. *Circ Res* **100**, 686–692.

Sheff DR, Daro EA, Hull M & Mellman I (1999). The receptor recycling pathway contains two distinct populations of early endosomes with different sorting functions. *J Cell Biol* **145**, 123–139.

Sheff D, Pelletier L, O'Connell CB, Warren G & Mellman I (2002). Transferrin receptor recycling in the absence of perinuclear recycling endosomes. *J Cell Biol* **156**, 797–804.

Simonsen A, Lippe R, Christoforidis S, Gaullier JM, Brech A, Callaghan J, Toh BH, Murphy C, Zerial M & Stenmark H (1998). EEA1 links PI_3K function to Rab5 regulation of endosome fusion. *Nature* **394**, 494–498.

Steele DF, Eldstrom J & Fedida D (2007). Mechanisms of cardiac potassium channel trafficking. *J Physiol* **582**, 17–26.

Ullrich O, Reinsch S, Urbe S, Zerial M & Parton RG (1996). Rab11 regulates recycling through the pericentriolar recycling endosome. *J Cell Biol* **135**, 913–924.

Van Wagoner DR, Pond AL, McCarthy PM, Trimmer JS & Nerbonne JM (1997). Outward K^+ current densities and Kv1.5 expression are reduced in chronic human atrial fibrillation. *Circ Res* **80**, 772–781.

Zerial M & McBride H (2001). Rab proteins as membrane organizers. *Nat Rev Mol Cell Biol* **2**, 107–117.

Acknowledgements

This study was supported by funding to D.F. from the Canadian Institutes for Health Research and the Heart and Stroke Foundation of British Columbia and the Yukon. We thank Dr Jodene Eldstrom for helpful comments on the manuscript and Kyung Hee Park and Fifi Chiu for excellent technical assistance.